

**Floodplain inundation analysis of the lower Guadalupe River:  
linking hydrology and floodplain-dependent resources**

Dr. Kimberly Meitzen  
Dr. Jennifer Jensen

Department of Geography  
Texas State University  
San Marcos, Texas

Dr. Thomas Hardy

Department of Biology  
Texas State University  
San Marcos, Texas

**Final Report Dated May 2018**  
**TWDB Contract No. 1448311791**  
**TPWD Contract No. 474120**

## **Introduction**

This project provides a set of deliverables for the Guadalupe River floodplain over a study area that spans from Gonzales to near Tivoli, Texas. The deliverables include five main components: 1) A Digital Terrain Model (DTM) for the floodplain study area developed at a 3-m horizontal scale; 2) Nine 3-m flood inundation raster maps representing flood stages for the 1 in 2-, 5-, 10-, 15-, 20-, and 50- year flood return periods and the National Weather Service minor, moderate, and major flood stages; 3) One polygon vector map of the floodplain coverage of the Texas Ecological Mapping Systems vegetation classification layer clipped to the floodplain study area; 4) Six habitat suitability models (HSMs) of Alligator Gar *Atractosteus spatula* spawning areas; and 5) A land use and land cover classification for 2004, 2008, and 2012 for the five counties (Calhoun, Victoria, Dewitt, Gonzales, and Refugio) covering the study area. This document describes the study area and the data sources, processing, and development of each of these main deliverables. Digital copies of these data layers accompany this document in an external hard drive.

## **Study Area**

The Guadalupe River arises in the Edwards Plateau where it drains highly dissected Cretaceous limestone in a regional landscape referred to as the Texas Hill Country. From here, it crosses the Balcones Escarpment into the Gulf Coastal Plain where it flows to the Guadalupe/San Antonio Bay and eventually to the Gulf of Mexico. Downstream of the escarpment the Guadalupe drains Tertiary and Quaternary coastal plain sedimentary units and flows through a broad, low-gradient, alluvial valley characterized by a wide floodplain (0.2-0.4 km).

This study focuses on the Guadalupe River in the coastal plain between Gonzales and Tivoli, which spans about a 257-km segment of the river (Figure 1). This segment of river is classified as a low-gradient alluvial meandering river with a topographically complex floodplain which contains numerous Pleistocene to Holocene-age geomorphic units, including abandoned channels, natural levee deposits, incised cutbanks, and pointbar meander scroll features. The 3-m spatial scale of the DTM and flood modeling were selected to capture this geomorphic variability, yet reasonably model this 257-km segment of river.

Alligator Gar is a floodplain-spawning fish within the lower Guadalupe River that we chose to use an example for developing a habitat suitability model (HSM) using the flood inundation maps supplemented with ecological data. Results from these analyses can inform agencies and stakeholders on the conservation and management of this species.

## **Project Deliverables**

### *1. Digital Terrain Model (DTM) Development*

Light Detection and Ranging (LiDAR) data for the Guadalupe River basin were acquired from the Texas Natural Resource Information System (TNRIS) for the various LiDAR project acquisitions

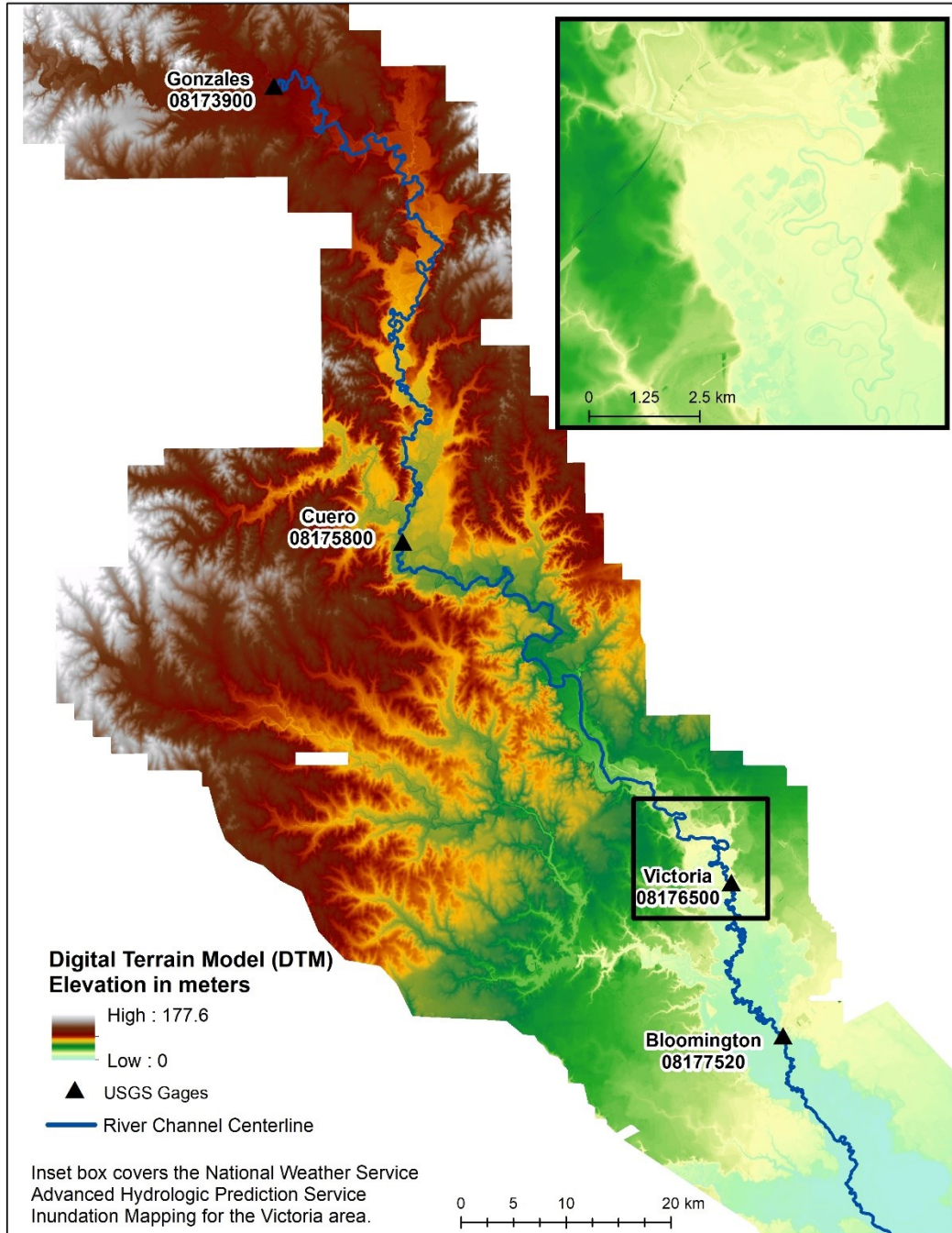


Figure 1: Guadalupe River floodplain study area.

for counties in the study area (Table 1). Most projects had .dem or .img hydro-enforced rasters. Hydrologic enforcement is the process of altering the elevation values in a DEM in order to ensure the continuous flow of water downstream. The simplest methods for filling sinks and assigning flow direction were enforced to the DTMs. However, for projects that only included classified LiDAR data, the Topo to Raster interpolation method in ArcMap was used to create the remaining digital terrain models (DTM). All LiDAR DTM tiles were projected to WGS 84, UTM Zone 14N; NAVD88 and mosaicked together at 3-m spatial resolution. Small gaps and negative blunders in

the LiDAR DTM warranted gap filling with USGS digital elevation model (DEM) 10 m products. The USGS DEMs were projected to UTM Zone 14N, resampled to 3 m, and merged with the LiDAR DTMs to create a continuous raster surface for the project. After gap filling, the DTM product was hydro-conditioned to fill spurious sinks in the dataset and double-checked for reasonable hydro-enforcement.

Table 1: County specific LiDAR acquisition dates.

<b>County</b>	<b>LiDAR Acquisition Dates</b>
Calhoun	December 9, 2010 – February 12, 2011
DeWitt	February 4-6, 2011; March 4, 2012; March 2-4, 2016
Gonzales	February 4 – March 6, 2011
Victoria	June 14-26, 2006

## 2. Floodplain Inundation Modeling

The floodplain inundation modeling used the USACE 1D/2D HEC-RAS (v. 5.0.1, USACE, 2016) and HEC-GeoRAS model (v. 10.2, USACE, 2016), HEC-SSP (v.2.1.1, USACE 2016), and ArcGIS 10.2 (ESRI, 2017). The primary inputs for the flood modeling include a DTM, discharge and stage data, flow resistance parameters, and boundary conditions relating the terrain model and river flow. Because of the size of the study area, the model was divided into four reaches defined by Guadalupe River USGS streamflow gages located proximal to Gonzales (gage ID 08173900), Cuero (gage ID 08175800), Victoria (gage ID 08176500), and Bloomington (gage ID 08177520). Reach-1 is between Gonzales and Cuero (111 km), Reach-2 is between Cuero and Victoria (83 km), Reach-3 is between Victoria and Bloomington (40 km), and Reach-4 is the remaining 23 km below Bloomington to just above the confluence with the Kuy Creek tributary (Figure 1).

The DTM described in section one (above) provided the terrain input data. All flood modeling was completed using the Guadalupe River at Victoria gage (08176500) as a reference. This gage included 82 annual peak flow events over the period 1935-2016. In total, we modeled nine discharge events. Three events were selected from the National Weather Service Advanced Hydrologic Prediction Service Inundation Mapping for the categories designated by minor ( $258 \text{ m}^3\text{s}^{-1}$ ), moderate ( $453 \text{ m}^3\text{s}^{-1}$ ), and major ( $885 \text{ m}^3\text{s}^{-1}$ ) flooding for the Victoria gage. The other six were selected from a flood frequency analysis for the Victoria gage. We used HEC-SSP to calculate flood recurrence intervals using the Bulletin 17B flow frequency analysis for 1 in 2-, 5-, 10-, 15-, 20-, and 50-year flood return period flood events (Figure 2 and Table 2).

We also compared pre- and post-Canyon Dam flood frequency return intervals, however the available USGS record for peak floods (1935-2016) does not include the historic flood events from 1869, 1913, 1921, 1929, or 1932; and we could not obtain published discharge values for these events to supplement the data record. By lacking these peak flow data points, the existing pre-dam annual peak flow record is not representative of the actual flood histories for the basin, and the analysis was skewed toward lower flood frequency discharges for the pre-dam flood probabilities calculations. Given this limitation we did not include that analysis in this report. Stage-discharge rating curves relating these flows to stage elevations for each gage site were used for the input boundary conditions to the flood modeling process.

Flow resistance parameters were defined using Manning’s ‘n’ roughness coefficients subjectively assigned relative to the land use code classes from the Ecological Mapping Systems of Texas data layer: barren (0.04), cultivated (0.075), forest (0.12), grassland 0.075), shrubland (0.085), urban (0.06), water/mainstem river (0.035), wetland (0.035).

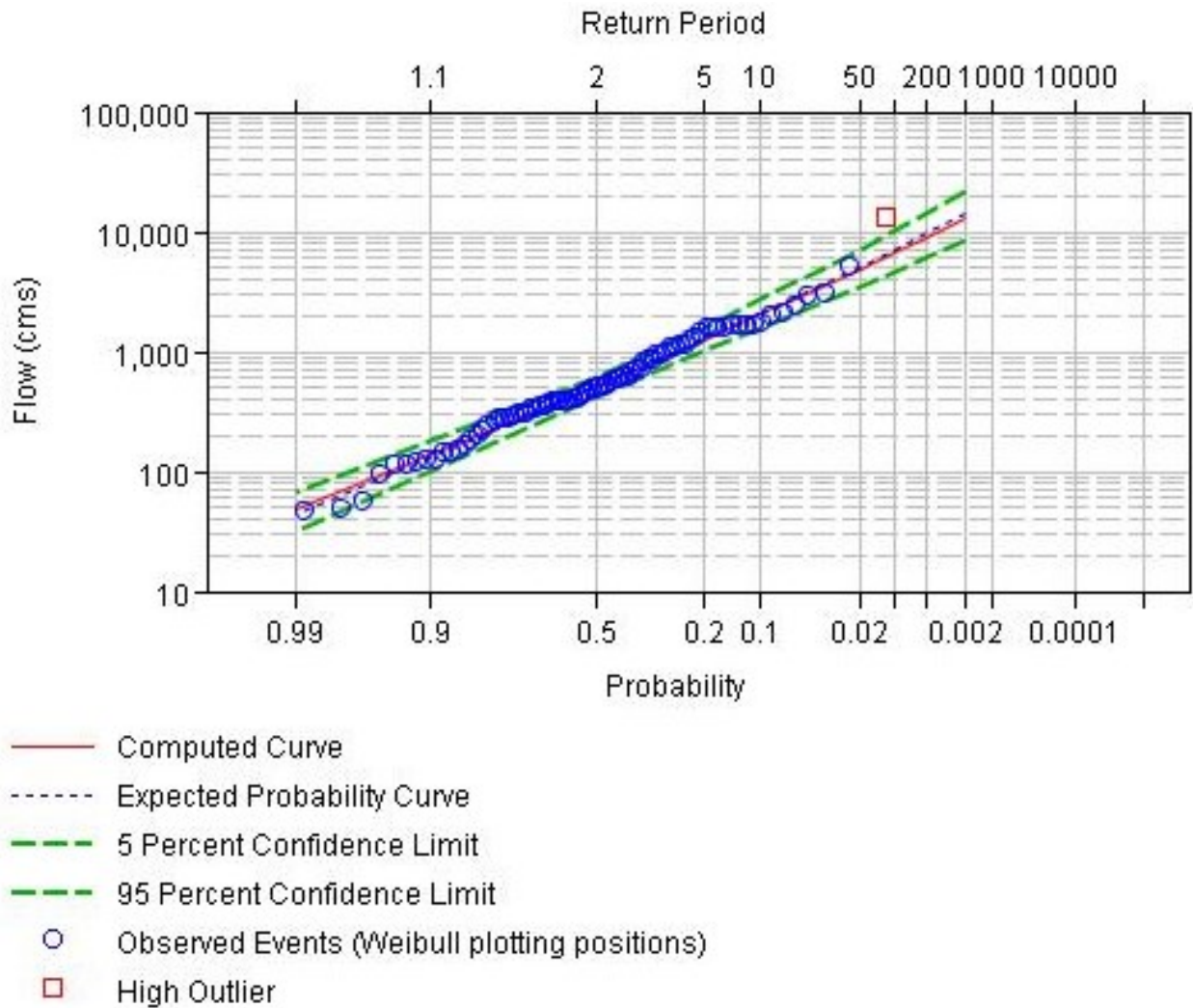


Figure 2: Bulletin 17B flood frequency curve for the Guadalupe River at Victoria, Texas, USGS gage 08176500.

Table 2: Flood frequency curve flow specifics for flood probabilities and recurrence intervals (RI).

Computed Curve (FLOW, m <sup>3</sup> s <sup>-1</sup> )	Expected Probability	Percent Chance Exceedance (RI Year)	Confidence Limits	
			0.05 (FLOW, m <sup>3</sup> s <sup>-1</sup> )	0.95 (FLOW, m <sup>3</sup> s <sup>-1</sup> )
4,863.90	5,129.60	2 (50)	7,194.00	3,548.90
3,057.60	3,159.90	5 (20)	4,272.00	2,324.80
2,602.20	2,674.40	6.67 (15)	3,568.30	2,004.90
2,035.70	2,078.00	10 (10)	2,716.90	1,598.10
1,252.80	1,266.10	20 (5)	1,595.60	1,013.70
505.7	505.7	50 (2)	614.1	416.1

The general workflow utilized for flood inundation modeling followed this sequence:

*A. Geometric Data Pre-Processing with HEC-GeoRAS (Steps 1-3):*

1. Divide the single DTM into the three DTMs based on the upper, middle, and lower reach boundaries. It was necessary to divide the model into these reaches given the size of the data files and processing limitations between ArcMap, HEC-GeoRAS, and HEC-RAS.

2. Develop geometric data for each of the reaches in ArcMap using HEC-GeoRAS toolbox. Geometric data includes the stream centerline, right and left bank lines, floodplain flowpath lines, cross-section cut lines, and landuse polygons (Figure 3). All geometric data layers were built into a geodatabase as feature class shapefiles. Geometric data development involved the following specifics:

- All cross-section lines cross the 500-year FEMA floodplain boundary. A total of 2,508 cross-section were generated, with an average spacing of about 100 m between cross-sections.
- Reach-1 is 111 km in length and contains 1,101 cross-sections.
- Reach-2 is 83 km in length and contains 832 cross-sections.
- Reach-3 is 40 km in length and contains 685 cross-sections.
- Reach-4 is 23km in length and contains 200 cross-sections.
- The land use layer was attributed with Manning’s ‘n’ values, and then this layer was intersected with the cross-section lines to attribute them with ‘n’ values.

3. Generate a HEC-GeoRAS export file of the geometric data for import into HEC-RAS.

*B. HEC-RAS Geometric Data QC and Flood Analyses (Steps 1-4):*

1. Import geometry from HEC-GeoRAS export file into HEC-RAS.

2. Digitally edit the geometric data in HEC-RAS to correct for errors generated during processing. Specific edits included the following:

- Adjusting bank station points so that they depict the correct location.

- Filter cross-section elevation points (the maximum allowed is 500 points per line, a filter is used to reduce the number of points given minimal changes in elevation along the line).
- QCing the Manning's 'n' values for the channel and floodplain. Only 20 values are allowed for each cross-section, therefore this involved subjectively merging some adjacent values based on cross section geometry and apparent landuse. We prioritized maintaining the difference between high and low values and preserving the 'n' values within the mainstem channel.

3. Perform steady state flow modeling based on two different types of boundary conditions. Water surface elevations from discharge and stage heights were used for the upstream and downstream boundary conditions in all cases except for the absolute lower end of the model where we used the estimated normal depth (measured channel slope of 0.0001). All flows were in m<sup>3</sup>/s and stage elevations in meters. Where results produced divided flow for a cross-section, the volume of flow removed from the mainstem channel was added back into the boundary conditions for the modeled profile. This occurred frequently in the lower portion of the model domain between Reach-3 and Reach-4 where there were many abandoned channels in the floodplain.

4. The final results of the modeling produced one dimensional water surface profiles for all 2,508 cross-sections for all nine modeled flows.

5. Generate export files for water surface profiles for all four reaches.

*C. Post-processing using HEC-GeoRAS and GIS to map 2D flood depths (Steps 1-5):*

1. Import water surface elevation profile data (attributed to cross-sections lines) for each modeled flood into ArcMap using the HEC-GeoRAS toolbox. Cross-section lines for each reach were merged into one shapefile for the whole study area. (Note: only step one used the HEC-GeoRAS tool, all other post-processing was completed using ESRI ArcMap tools).

2. Generate spatially-explicit 2D water surface elevation TIN layer, convert the TIN layer to a 3m water surface elevation grid and difference this grid with the DTM to create 3m flood inundation depth rasters for the full study area.

3. Flood depth rasters were processed to include only the inundated areas that were structurally connected to the main stem river channel. We used the 'region group' tool in ArcMap Spatial Analyst and set parameters to include all inundated cells that were adjacent to, shared a side boundary, or were linked by a diagonal corner. All other cells were excluded and removed from the final raster. This step ensured that 'ponded' water not hydraulically connected to the mainstem as an artifact of topography were removed.

5. Steps 2-4 were completed for all nine discharge events.

6. The results of this process include nine spatially explicit 3m flood inundation depth rasters that seamlessly cover the entire study area (Figures 4-12).

The 2-year flood inundates low lying areas of the floodplain and has the greatest overbank extent in the lower study reaches (Figure 6). The 5-year flood inundates more extensively into the floodplain and low-lying areas throughout the upper and lower reaches (Figure 8). The 10-year flood produces more extensive overbank inundation but does not completely inundate the entire floodplain (Figure 9). There is minimal change in the area of inundation between the 15- and 20-

year flood and although the 20-year flood does not inundate the entire floodplain, it is more extensive with increased flood depths (Figure 10 and 11). The 50-year flood is associated with the greatest inundation extent and deepest inundation depths (Figure 12).

A caveat of the flood inundation model is that we do not have validation data distinct from the USGS stage heights. An error analysis comparing the modeled water surface elevations with USGS stage-discharge water surface elevations for the channel yielded minimal error (Table 3).

Table 3: Error analysis showing the difference between the USGS water surface elevations for each gage and the modeled water surface elevations. USGS water surface elevations were measured by adding the stage for the corresponding discharge to the gage datum.

	<b>Gonzales 08173900</b>			<b>Cuero 08175800</b>		
<b>Event (cms)</b>	model (m)	USGS	diff (m)	model (m)	USGS	diff (m)
NWS minor (257)	78.23	78.27	-0.04	44.91	44.96	-0.05
NWS moderate (453)	80.65	80.71	-0.06	46.68	46.63	0.05
2-year (506)	81.08	81.02	0.06	47.26	47.24	0.02
NWS major (884)	82.87	82.84	0.03	48.88	48.92	-0.04
5-year (1260)	83.50	83.45	0.05	49.78	49.83	-0.05
10-year (2057)	84.07	84.06	0.01	50.85	50.90	-0.05
15-year (2638)	84.31	84.37	-0.06	51.30	51.36	-0.06
20-year (3108)	84.45	84.52	-0.07	51.51	51.51	0.00
50-year (4997)	84.66	84.67	-0.01	51.71	51.66	0.05
	<b>Victoria 08176500</b>			<b>Bloomington 08188800</b>		
<b>Event (cms)</b>	model (m)	USGS	diff (m)	model (m)	USGS	diff (m)
NWS minor (257)	15.30	15.28	0.02	7.50	7.50	0.00
NWS moderate (453)	17.01	17.03	-0.02	7.91	7.90	0.01
2-year (506)	17.30	17.20	0.10	8.02	8.00	0.02
NWS major (884)	17.83	17.80	0.03	8.18	8.10	0.08
5-year (1260)	17.93	17.90	0.03	8.26	8.25	0.01
10-year (2057)	18.04	18.00	0.04	8.58	8.60	-0.02
15-year (2638)	18.13	18.10	0.03	8.72	8.70	0.02
20-year (3108)	18.22	18.20	0.02	8.90	8.90	0.00
50-year (4997)	18.58	18.50	0.08	9.55	9.50	0.05

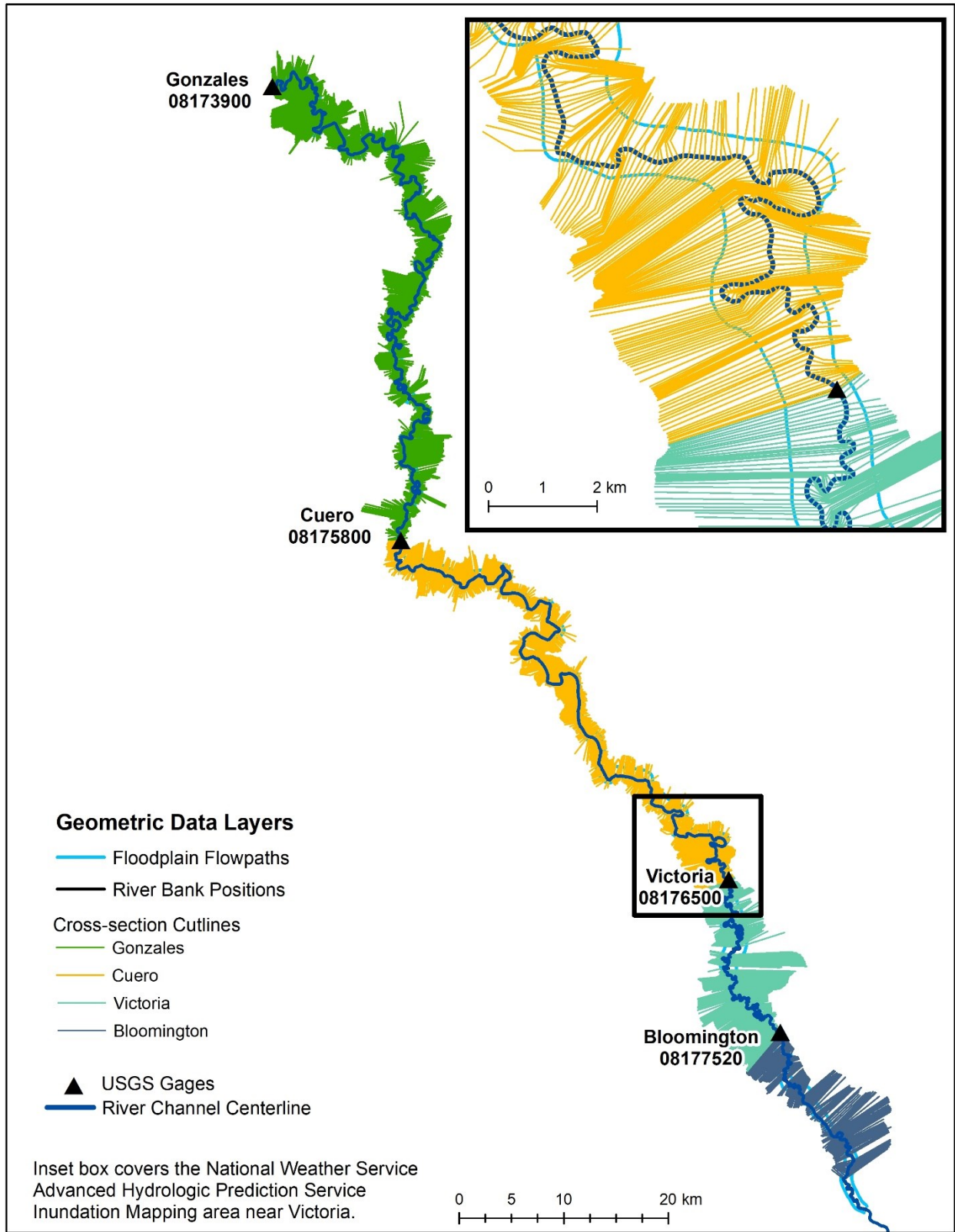


Figure 3: Geometry layers created in ArcMap from HEC-GeoRAS toolbox.

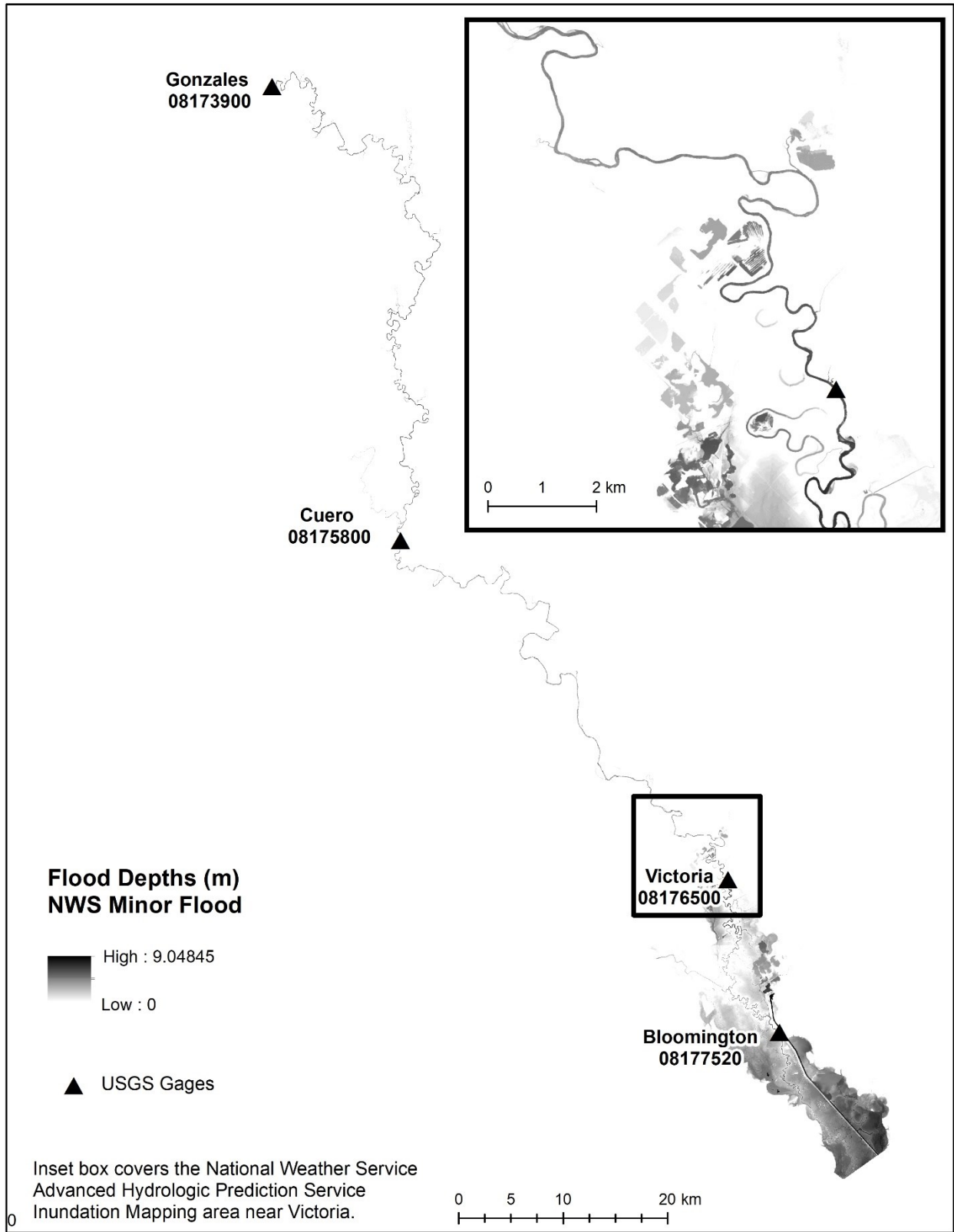


Figure 4: Flood inundation map for NWS minor flood.

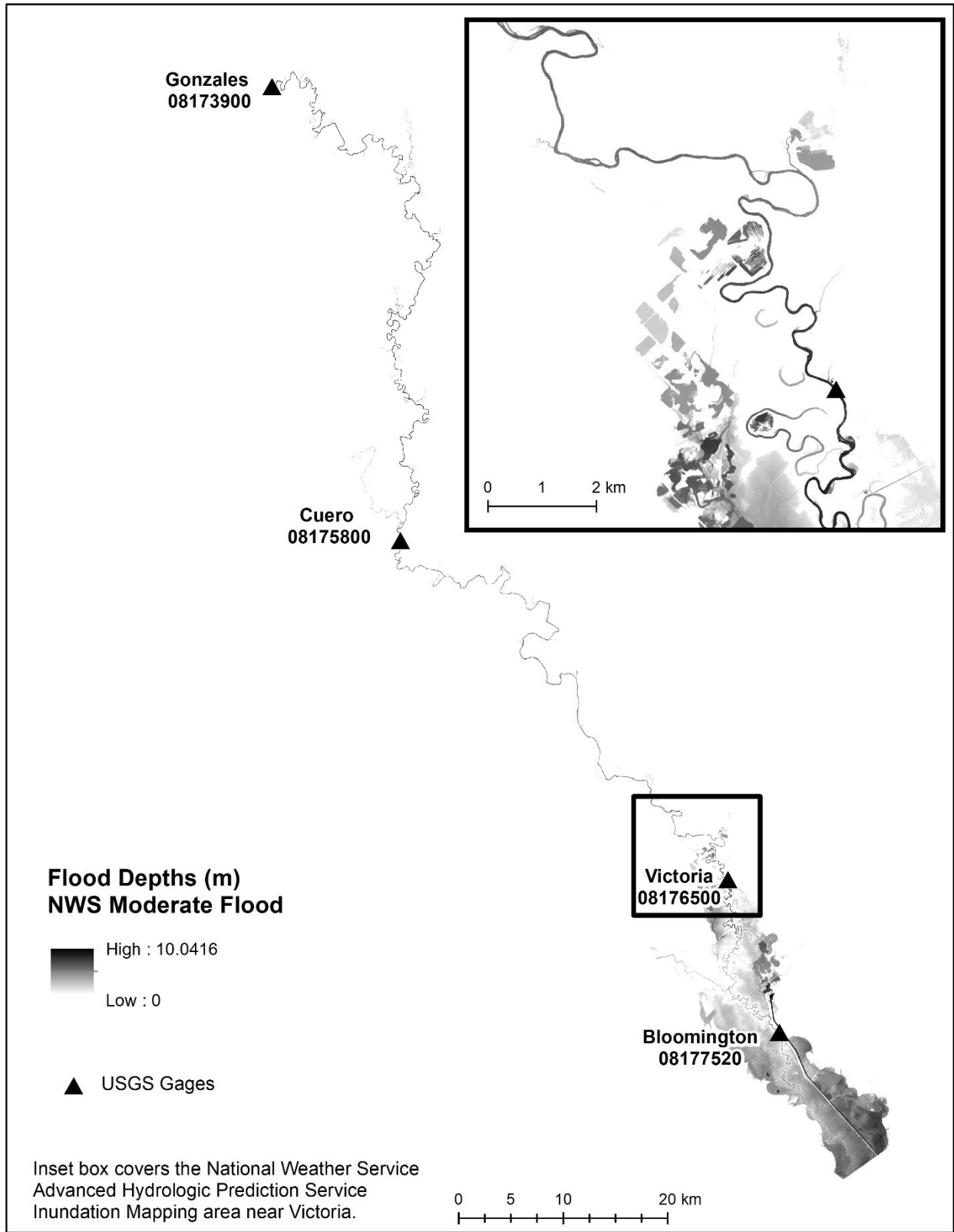


Figure 5: Flood inundation map for NWS moderate flood.

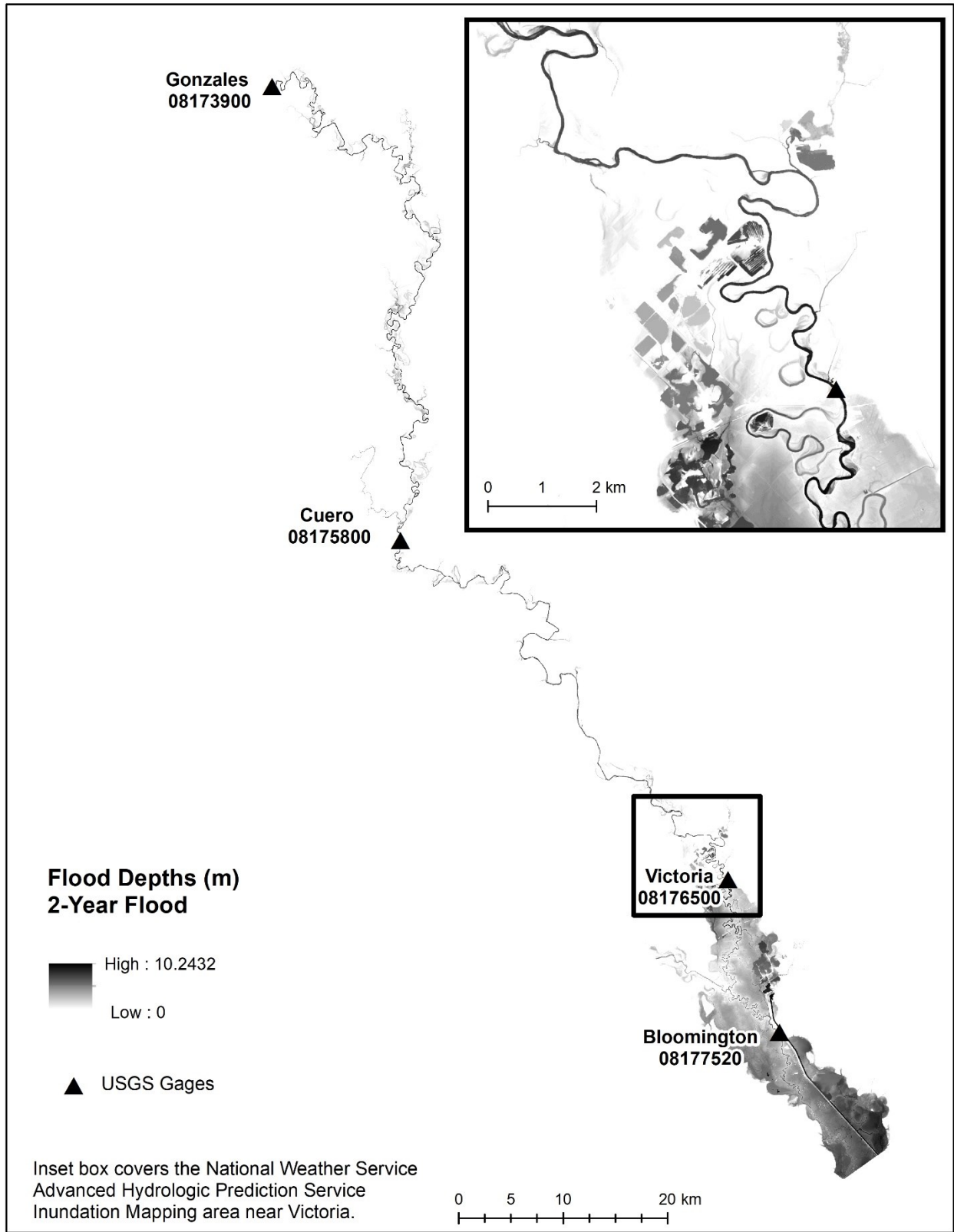


Figure 6: Flood inundation maps for 2-year flood.

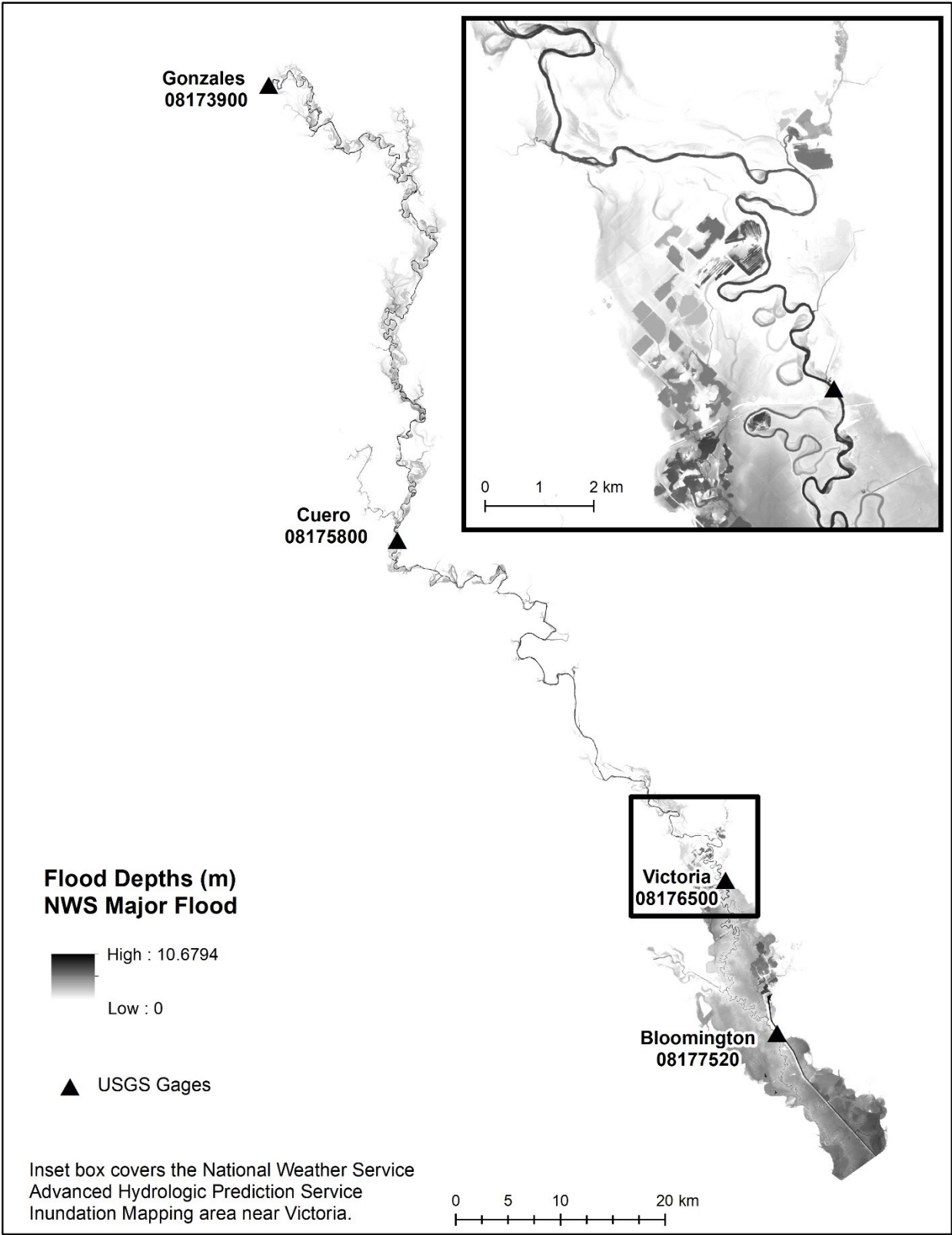


Figure 7: Flood inundation map for NWS major flood.

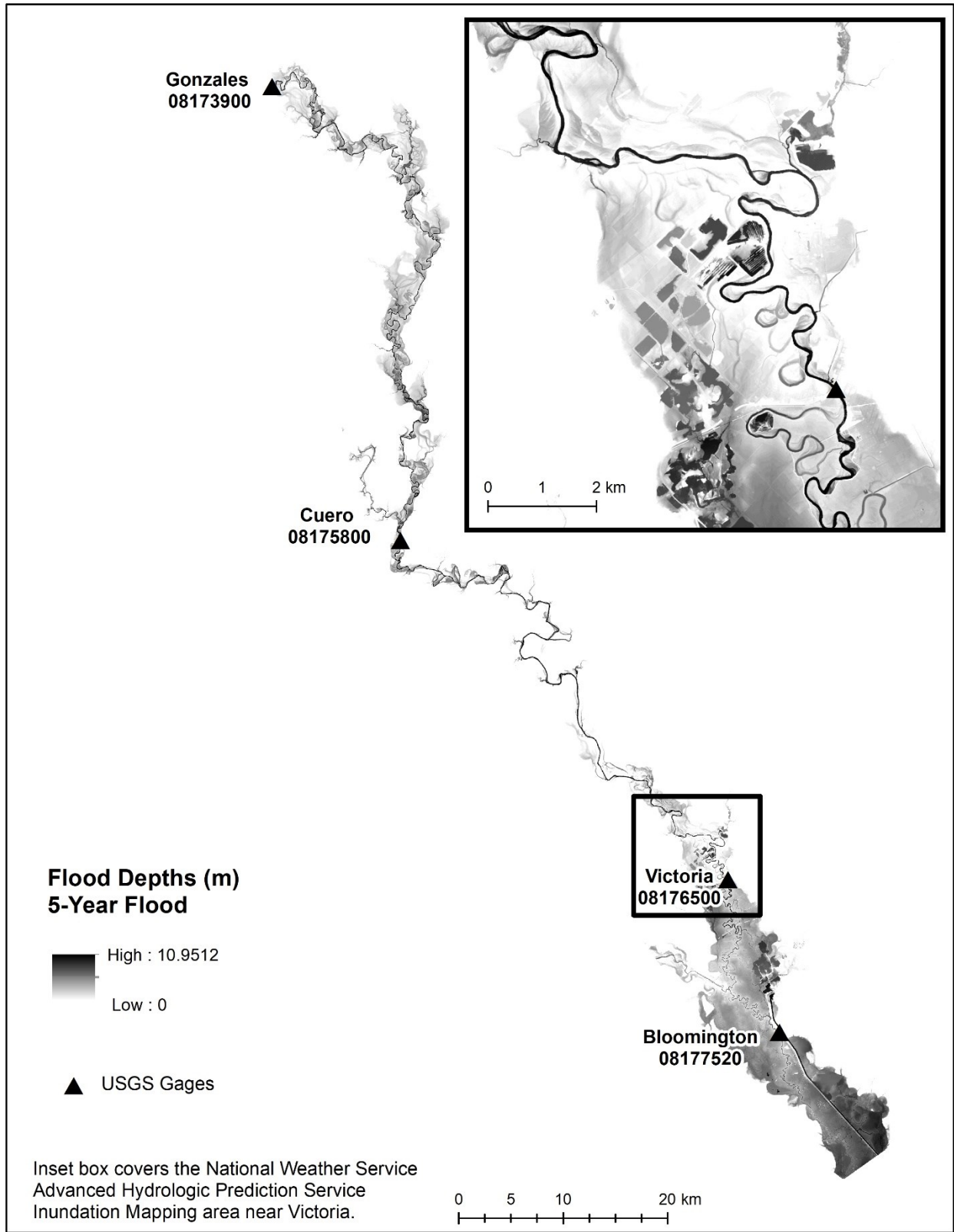


Figure 8: Flood inundation maps for 5-year flood.

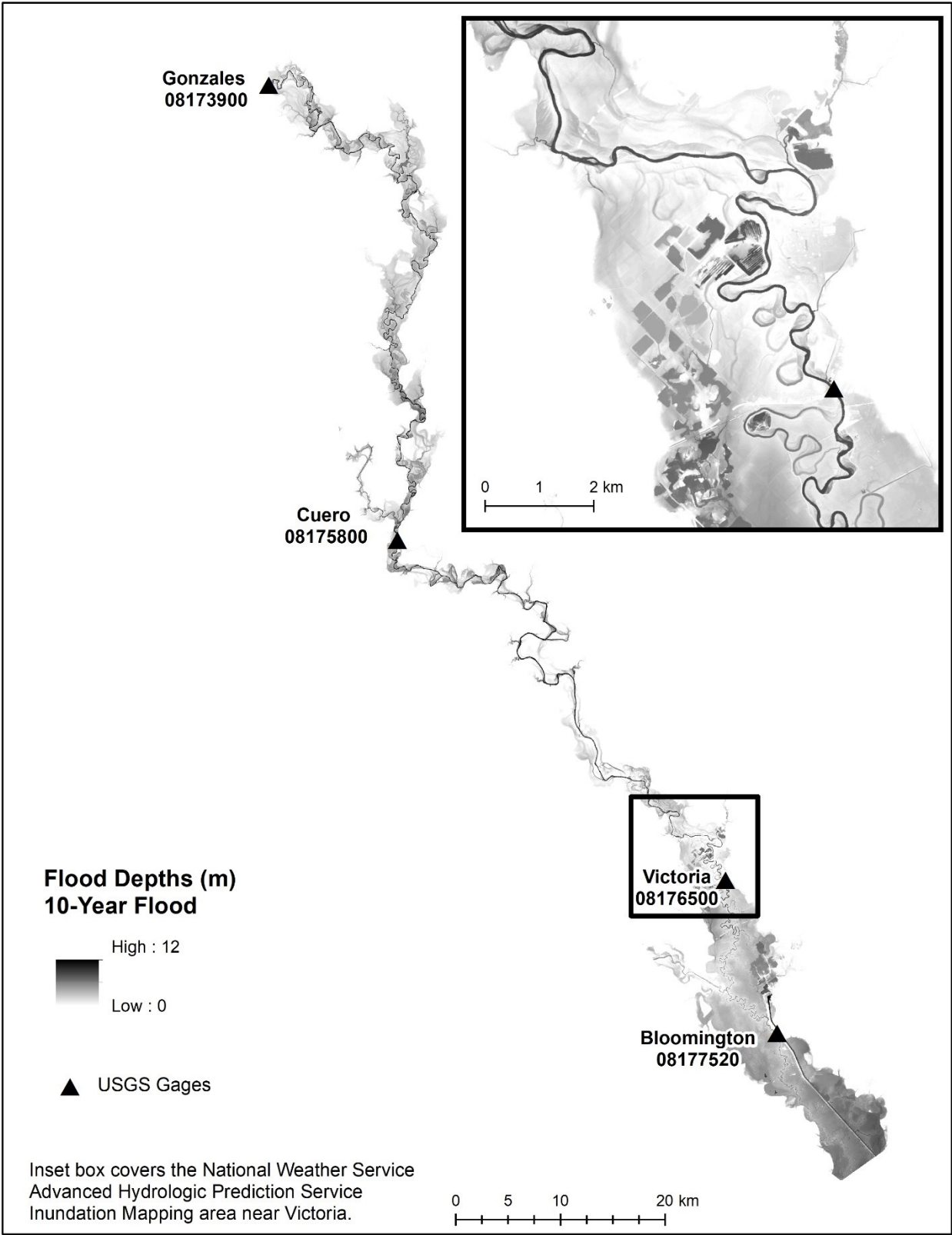


Figure 9: Flood inundation maps for 10-year flood.

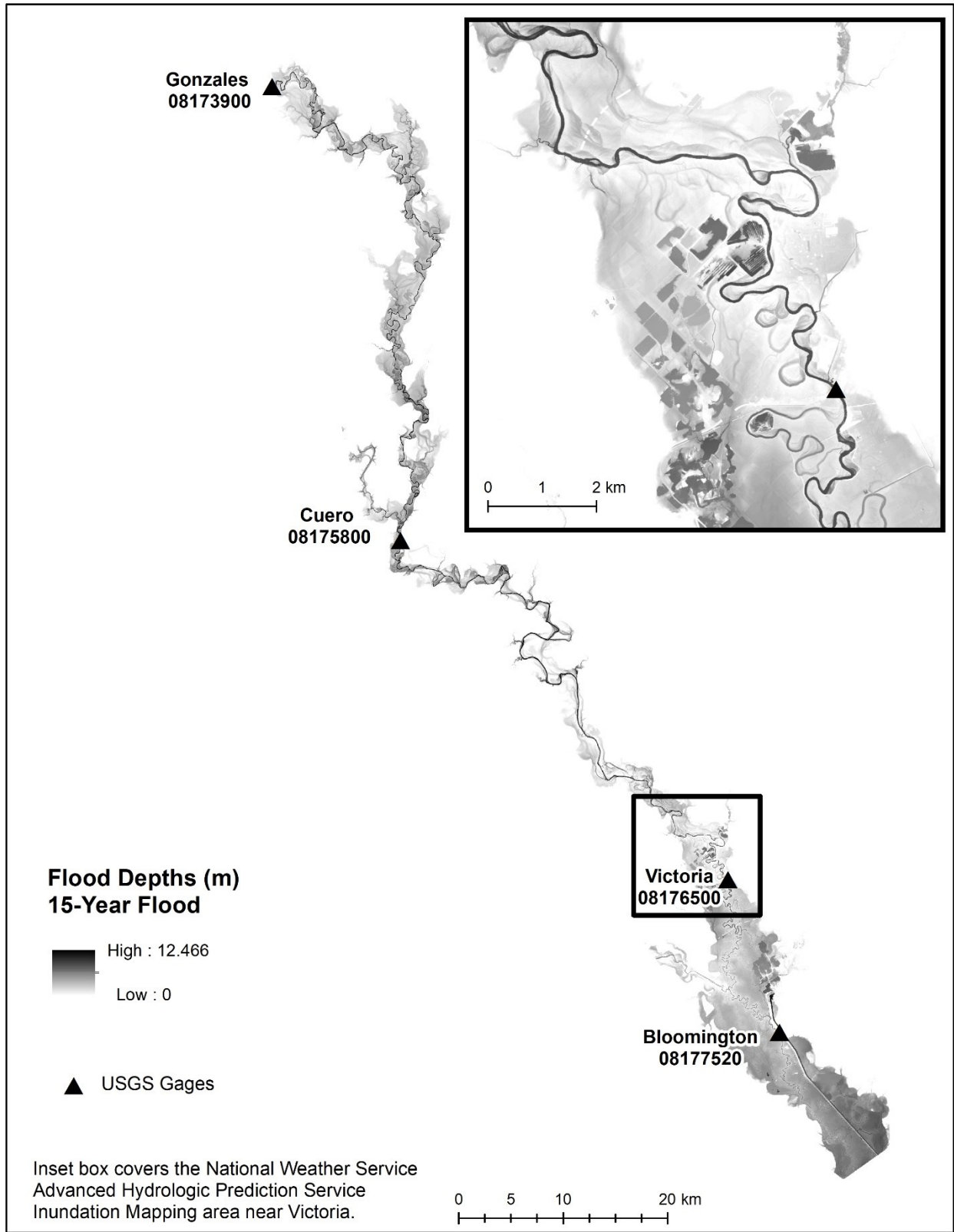


Figure 10: Flood inundation maps for 15-year flood.

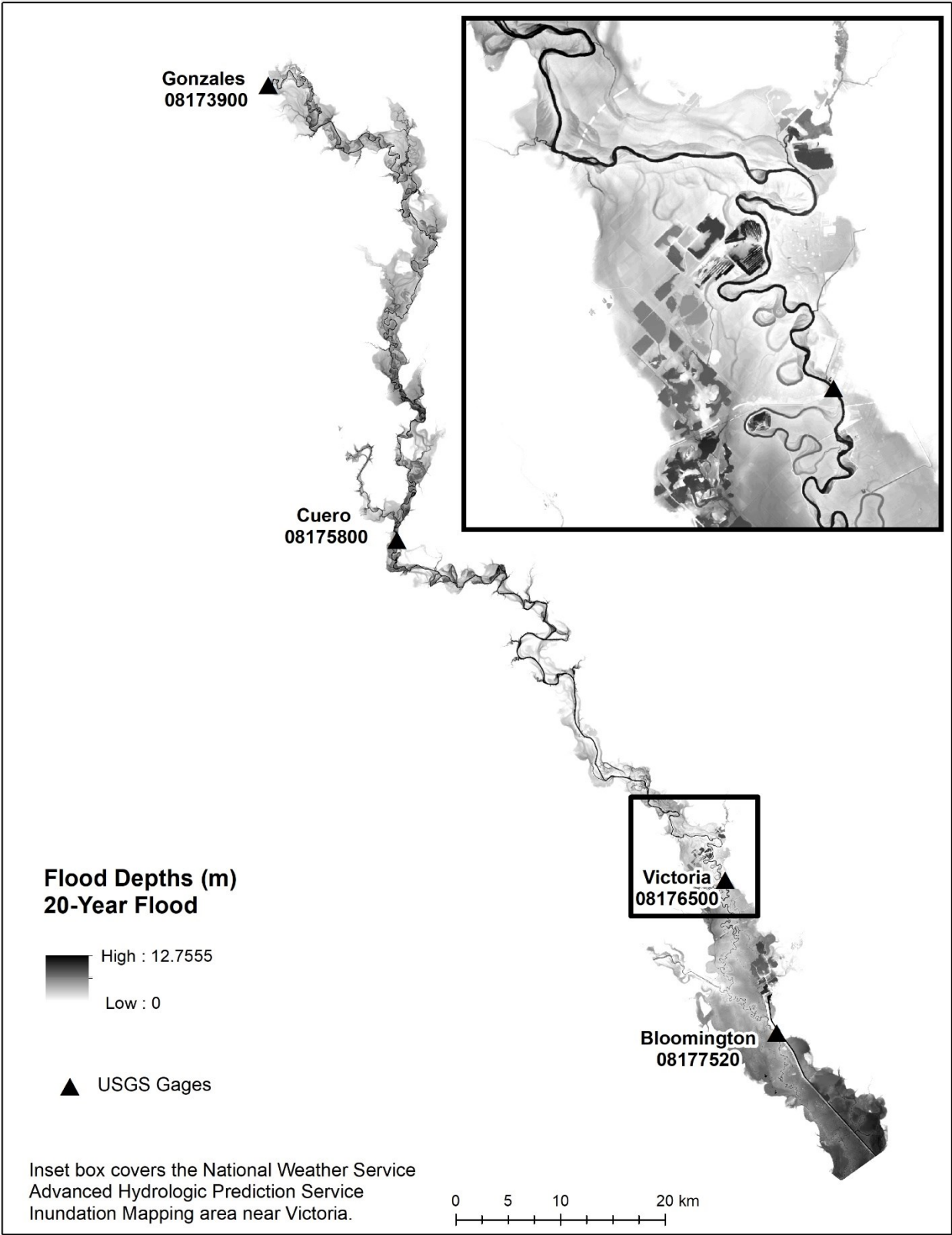


Figure 11: Flood inundation maps for 20-year flood.

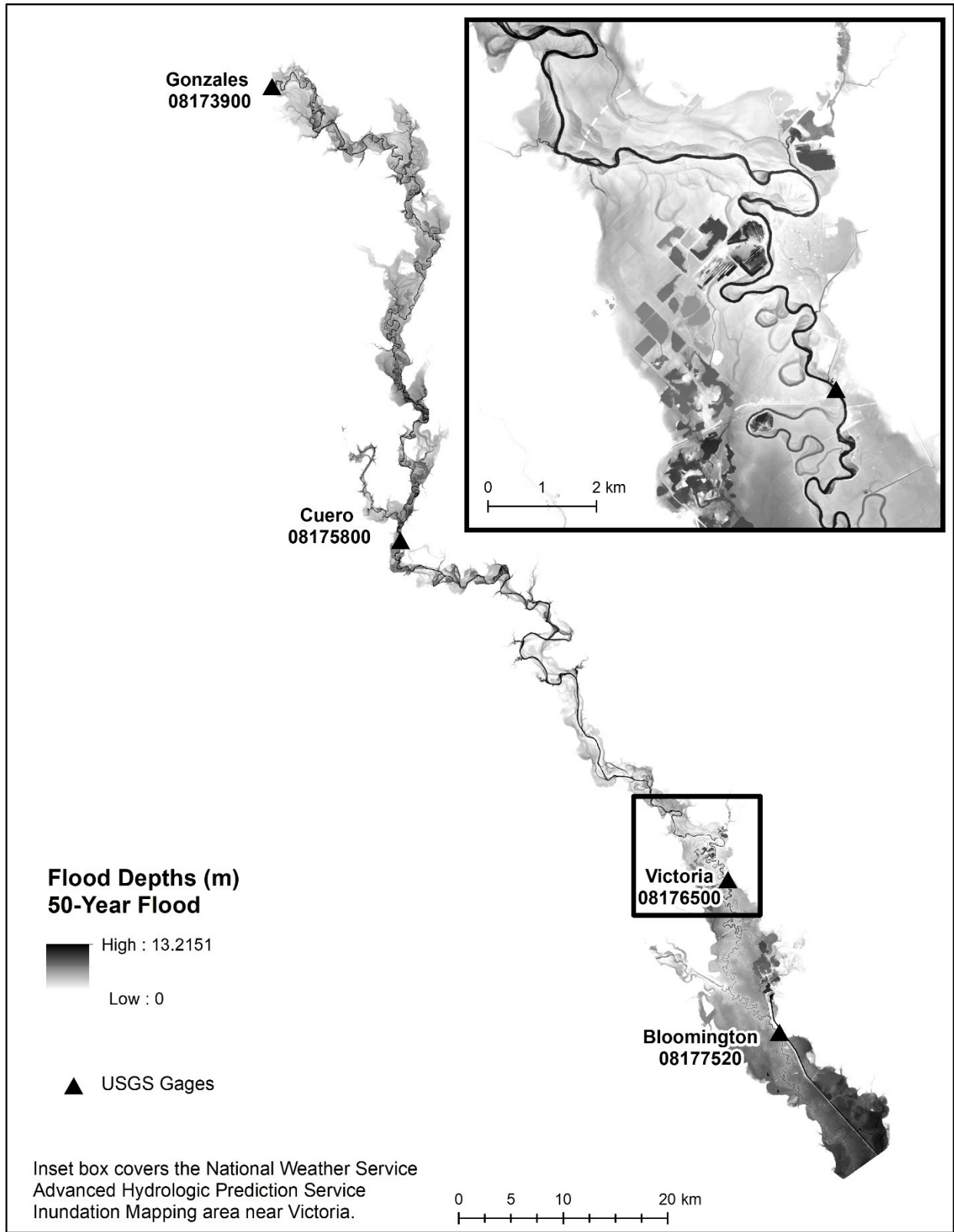


Figure 12: Flood inundation maps for 50-year flood.

### 3. Texas Ecological Mapping Systems data clipped to the 500-year FEMA floodplain

In addition to the flood inundation depth maps and HSMs, we also included the vector polygon layer of the Texas Ecological Mapping Systems data clipped to the 500-year FEMA floodplain boundary. We used this dataset layer to assign the Manning’s ‘n’ values to the different vegetation cover types for the flood modeling and as the base layer that was reclassified to assign suitable vegetation types for Alligator Gar spawning as noted below.

### 4. Habitat Suitability Modeling

We developed a habitat suitability model (HSM) for Alligator Gar spawning areas using the flood inundation model outputs and the Texas Ecological Mapping Systems data. We reclassified these data layers to represent only the criteria specific to their spawning preferences and modeled the areas of suitable spawning. Texas Parks and Wildlife Department staff provided the habitat suitability criteria (Clint Robertson, personal communication). The criteria included flood depths within the range of 0.2–2 m and 46 vegetation communities within the designated floodplain study area (Table 3).

Table 3: Vegetation communities derived from the Texas Ecological Mapping Systems data classified as suitable for Alligator Gar *Atractosteus spatula* spawning.

Vegetation Community Common Names	
Central Texas: Floodplain Deciduous Shrubland	Blackland Prairie: Disturbance or Tame Grassland
Central Texas: Floodplain Evergreen Shrubland	Gulf Coast: Coastal Prairie
Central Texas: Floodplain Herbaceous Vegetation	Gulf Coast: Coastal Prairie Pondshore
Central Texas: Floodplain Herbaceous Wetland	Gulf Coast: Salty Prairie
Central Texas: Riparian Deciduous Shrubland	Gulf Coast: Salty Prairie Shrubland
Central Texas: Riparian Evergreen Shrubland	Inland: Salty Prairie
Central Texas: Riparian Herbaceous Vegetation	Inland: Salty Prairie Shrubland
Central Texas: Riparian Herbaceous Wetland	Invasive: Evergreen Shrubland
Coastal and Sandsheet: Deep Sand Grassland	Marsh
Coastal and Sandsheet: Deep Sand Shrubland	Native Invasive: Baccharis Shrubland
Coastal Bend: Floodplain Deciduous Shrubland	Native Invasive: Common Reed
Coastal Bend: Floodplain Evergreen Shrubland	Native Invasive: Juniper Shrubland
Coastal Bend: Floodplain Grassland	Native Invasive: Mesquite Shrubland
Coastal Bend: Floodplain Herbaceous Wetland	Non-native Invasive: Saltcedar Shrubland
Coastal Bend: Riparian Deciduous Shrubland	Post Oak Savanna: Live Oak Shrubland
Coastal Bend: Riparian Evergreen Shrubland	Post Oak Savanna: Sandyland Grassland
Coastal Bend: Riparian Grassland	Post Oak Savanna: Savanna Grassland
Coastal Bend: Riparian Herbaceous Wetland	Row Crops
Coastal Plain: Terrace Sandyland Grassland	South Texas: Clayey Blackbrush Mixed Shrubland
Coastal: Salt and Brackish High Tidal Marsh	South Texas: Clayey Mesquite Mixed Shrubland
Coastal: Salt and Brackish High Tidal Shrub Wetland	South Texas: Shallow Dense Shrubland
Coastal: Salt and Brackish Low Tidal Marsh	South Texas: Shallow Shrubland
Coastal: Sea Ox-eye Daisy Flats	South Texas: Shallow Sparse Shrubland

We conducted all habitat suitability modeling within ArcMap 10.5.1, using raster datasets reclassified to binary conditions to assign suitable and non-suitable conditions for the flood depths and vegetation data sets. Initially we produced HSMs that yielded only the suitable areas that showed agreement between both the flood depths and the vegetation classes, however after reviewing the results against satellite imagery, we noticed several places where the vegetation classes were misclassified and the actual land cover type was suitable for spawning. For this reason, we included habitat suitability for four conditional criteria.

The four conditional statements to calculate suitability criteria included: (1) suitable for flood depth and vegetation land cover, (2) suitable for flood depth and unsuitable for vegetation land cover, (3) unsuitable for flood depth and suitable for vegetation land cover, and (4) unsuitable flood depth and unsuitable land cover. This information may be useful for future analysis involving a different land cover dataset or during field reconnaissance for spawning fish.

The main stem river channel was removed from the final layers to include only floodplain areas. A summary of suitable habitat for flood depths and vegetation land cover for Alligator Gar spawning habitat area as an independent variable against discharge yields a non-linear relationship, with the greatest amount of suitable habitat area occurring in the range of 1,000–5,000 m<sup>3</sup>s<sup>-1</sup> (Figure 13). Mapped outputs for the four conditional criteria provide spatially-explicit examples of the suitable habitat relative to flood recurrence intervals (Figures 14-22).

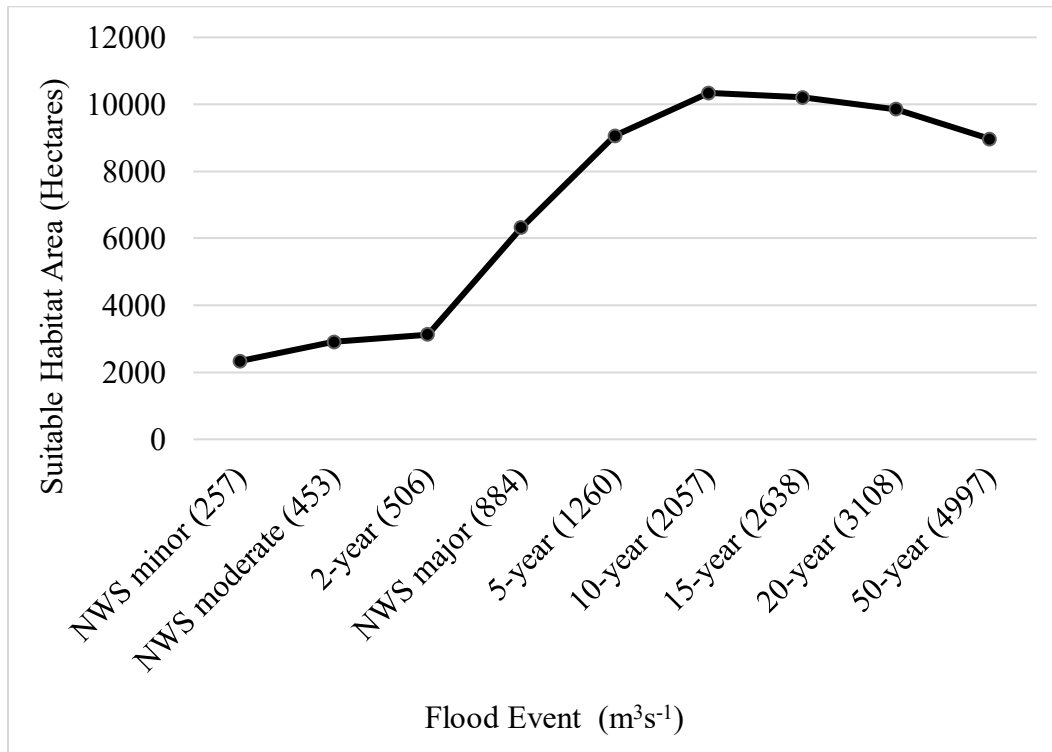


Figure 13: Area of suitable spawning habitat for flood depth and vegetation criteria for Alligator Gar relative to discharge.

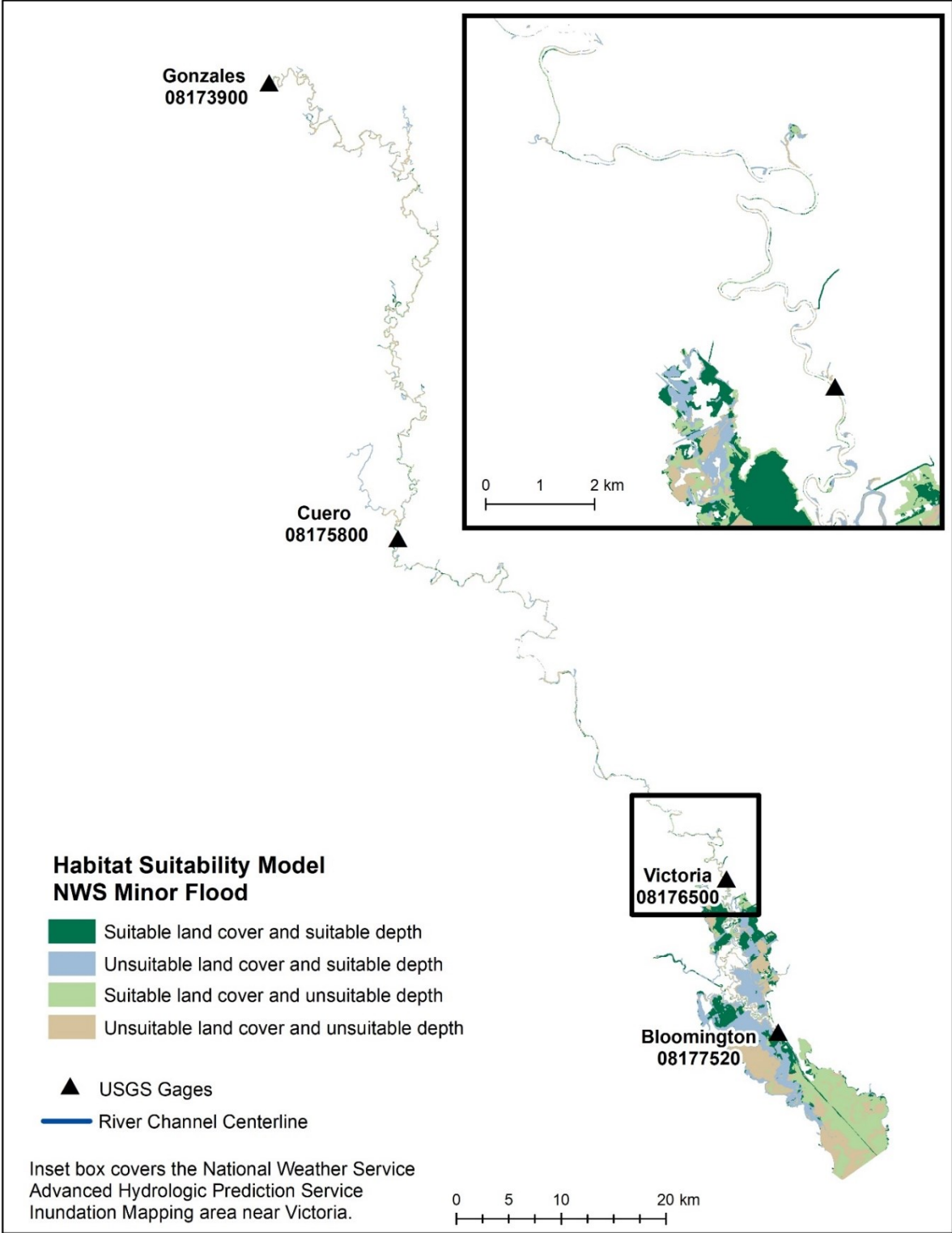


Figure 14: Habitat suitability map for the NWS minor flood.

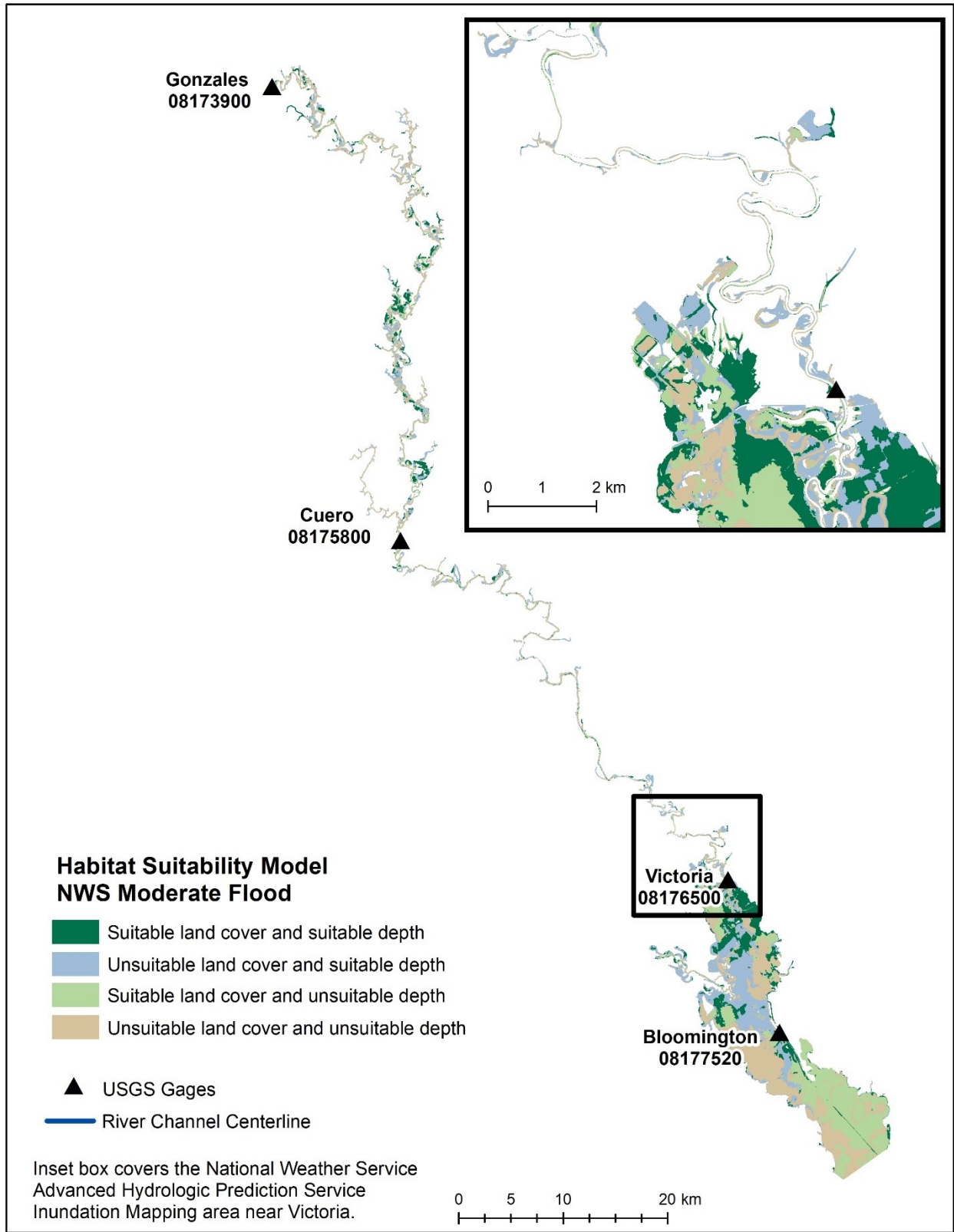


Figure 15: Habitat suitability map for the NWS moderate flood.

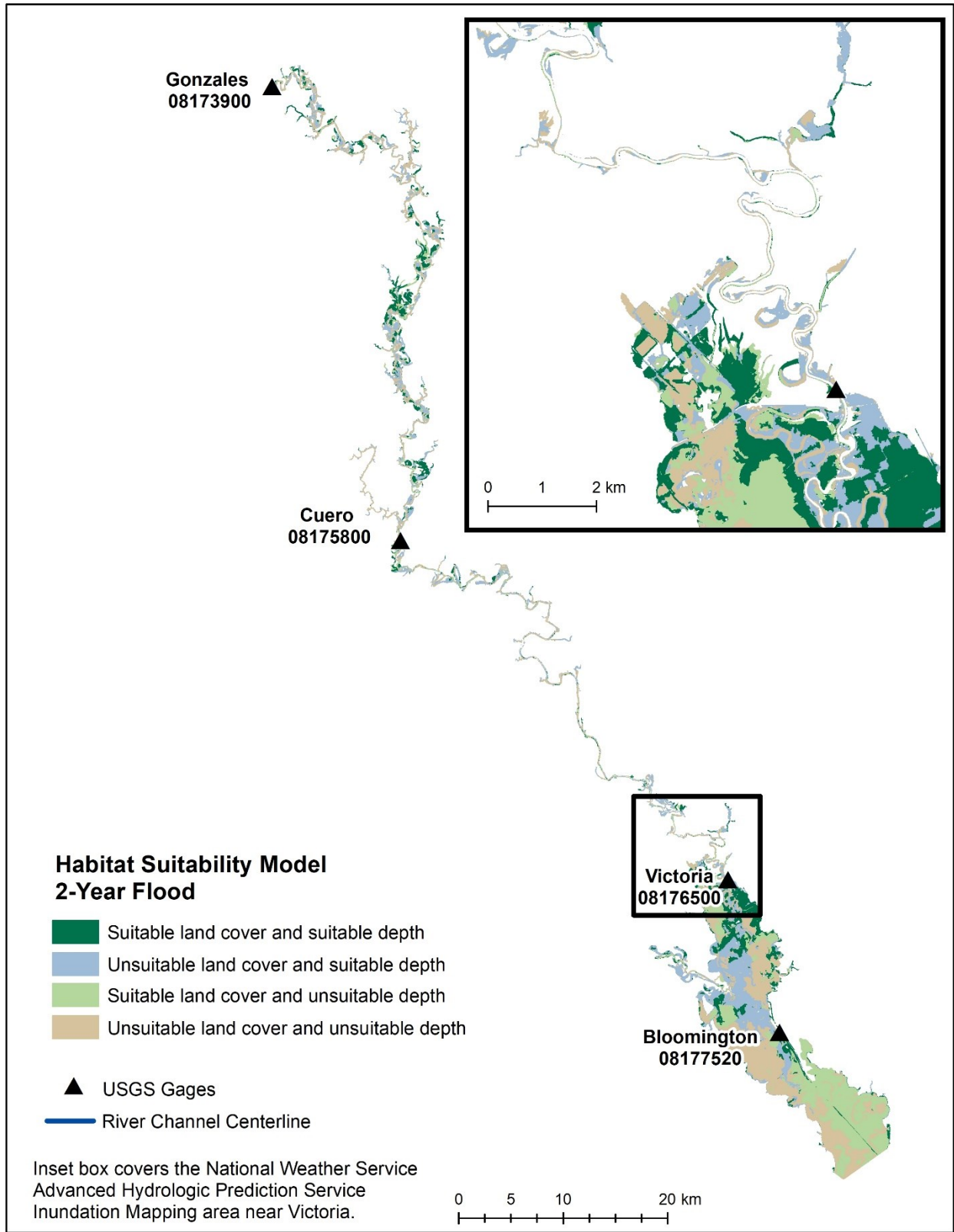


Figure 16: Habitat suitability map for the 2-year flood recurrence interval.

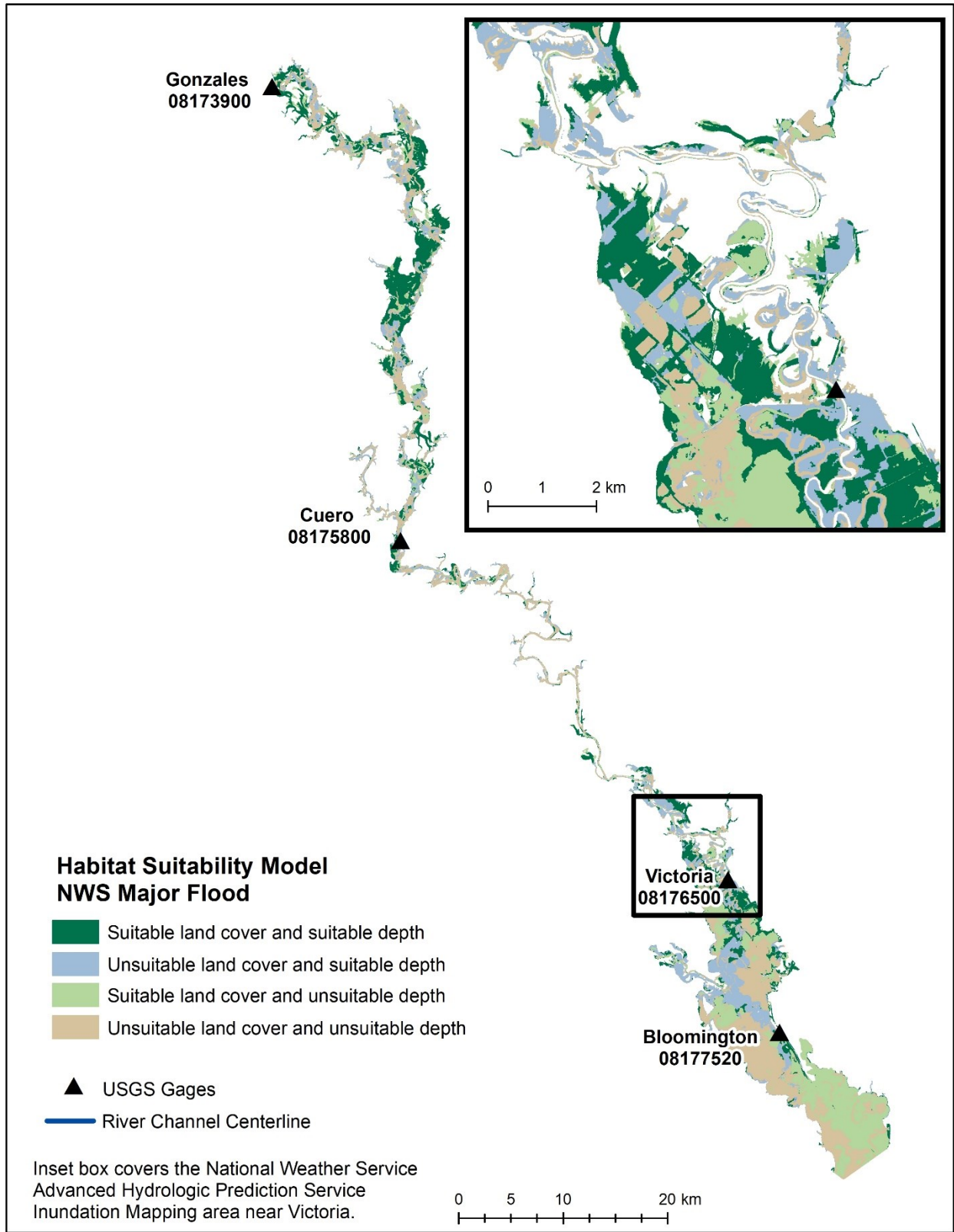


Figure 17: Habitat suitability map for the NWS major flood.

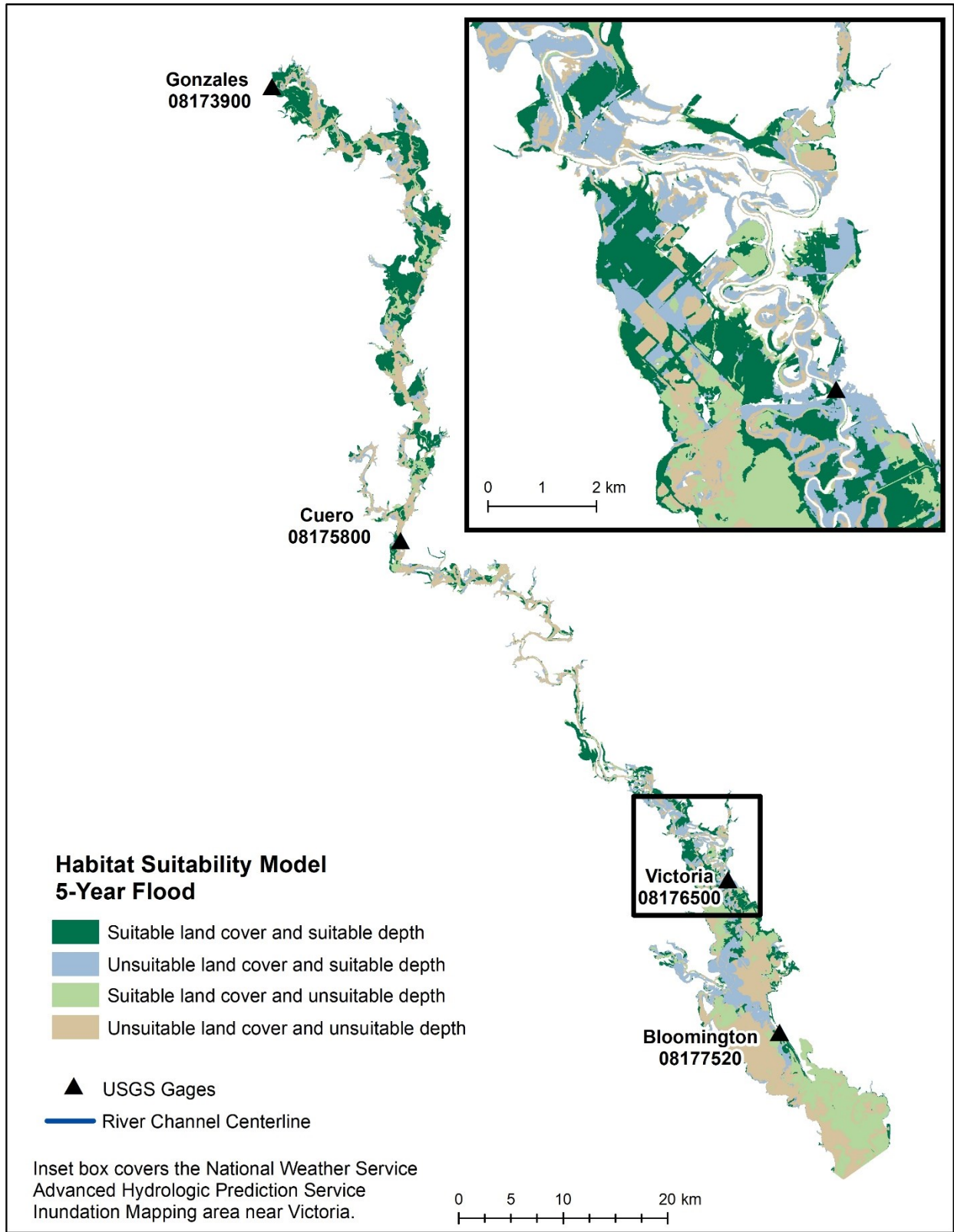


Figure 18: Habitat suitability map for the 5-year flood recurrence interval.

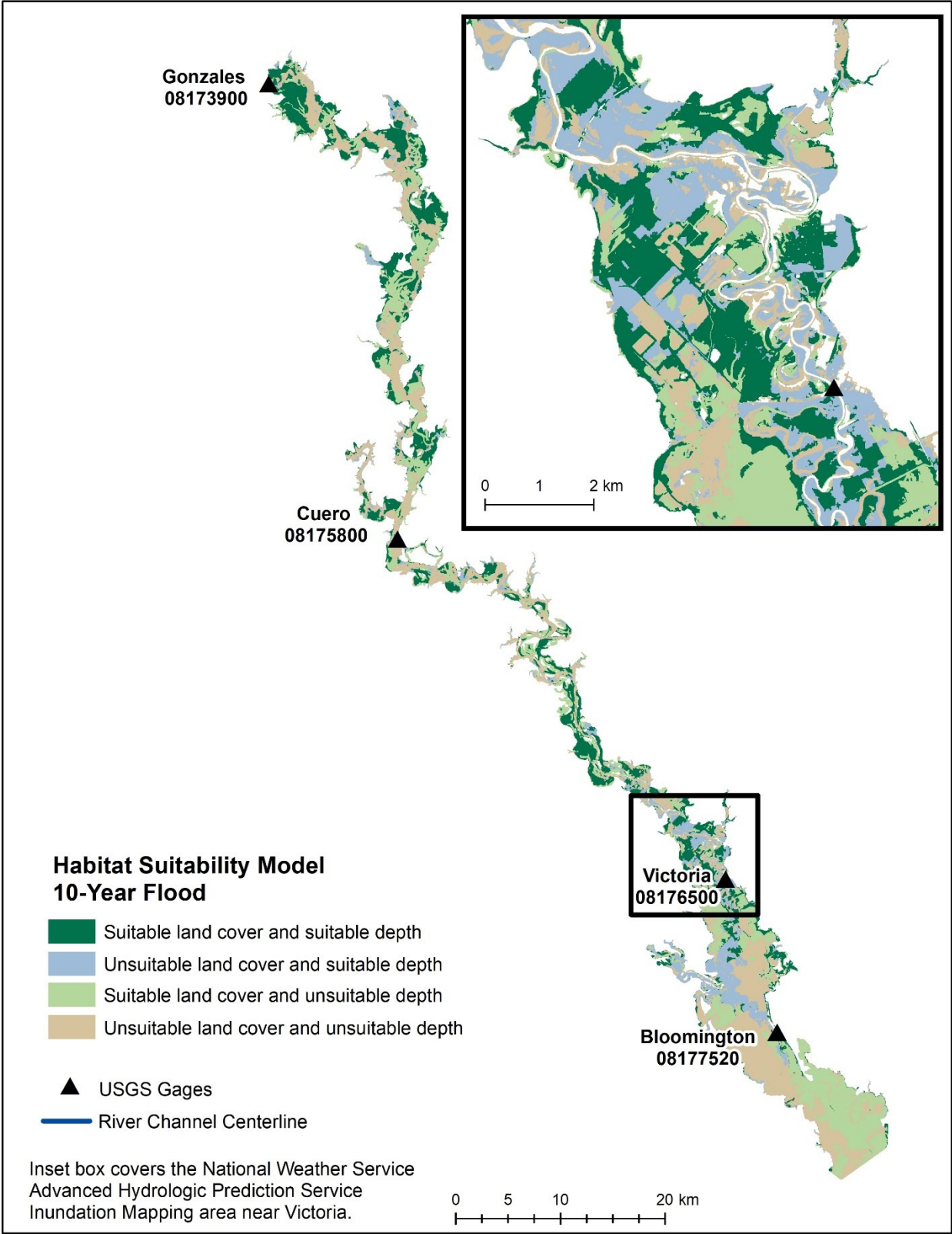


Figure 19: Habitat suitability map for the 10-year flood recurrence interval.

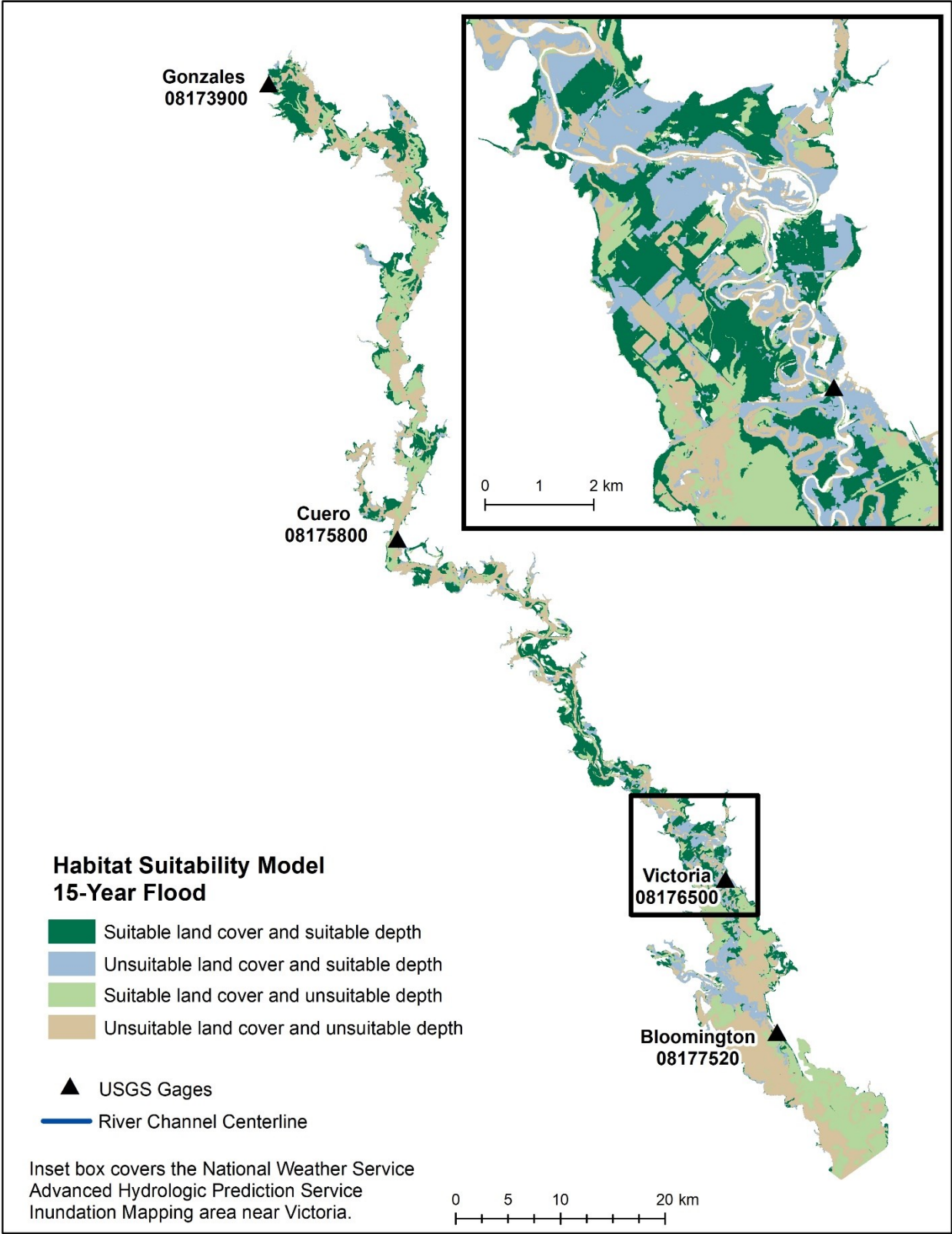


Figure 20: Habitat suitability map for the 15-year flood recurrence interval.

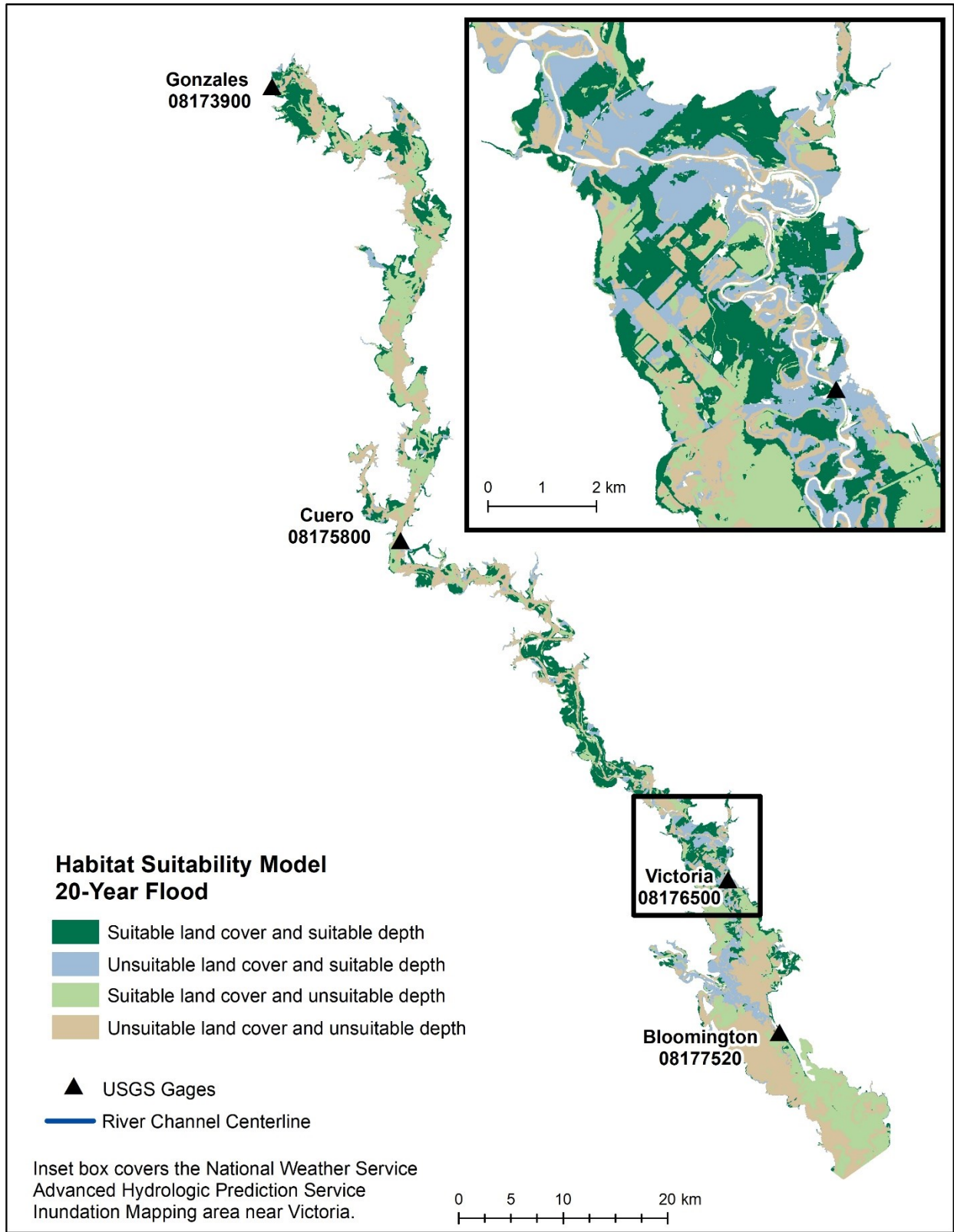


Figure 21: Habitat suitability map for the 20-year flood recurrence interval.

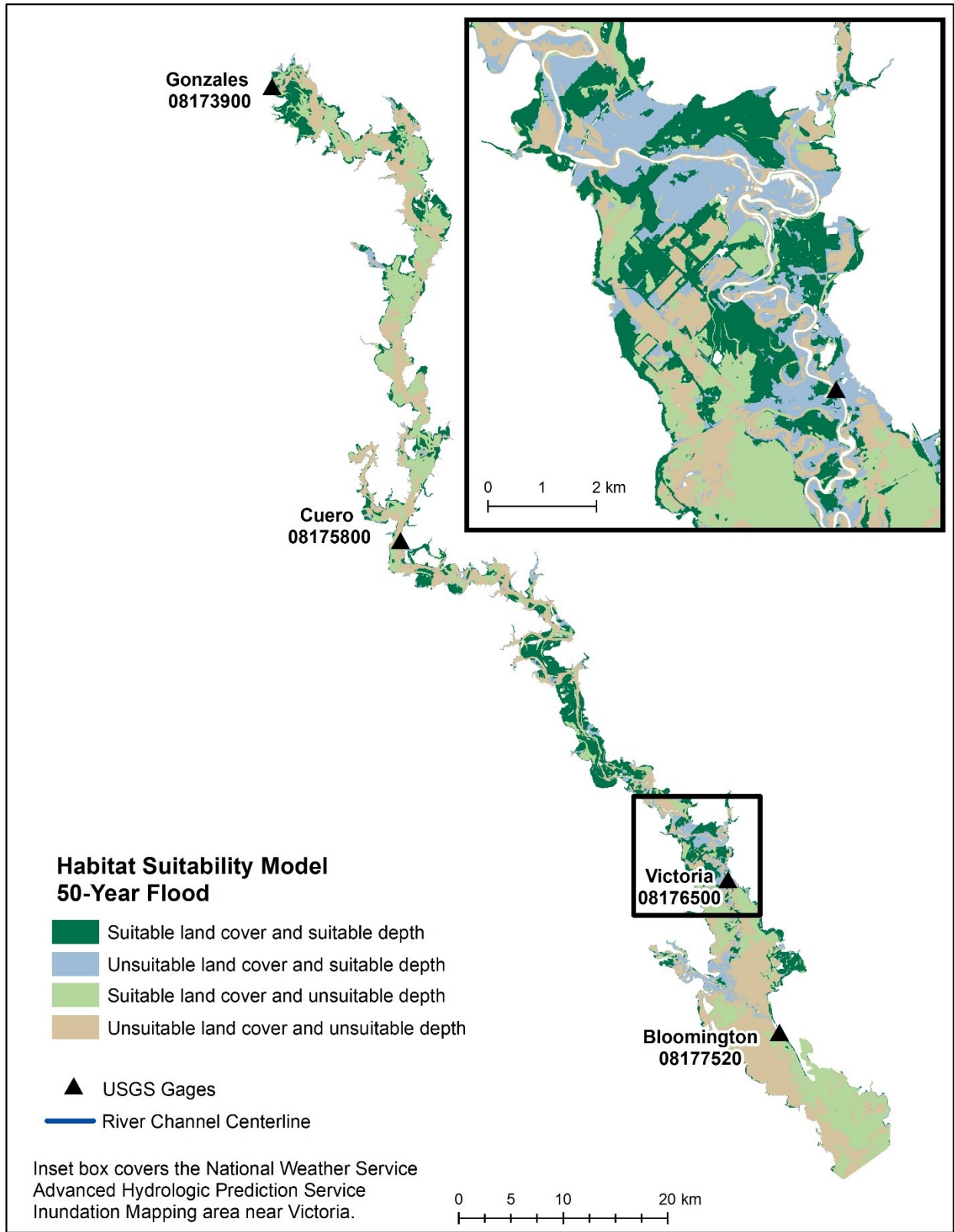


Figure 22: Habitat suitability map for the 50-year flood recurrence interval.

## 5. Land Cover Classification

Although not part of the original scope of work, high resolution land cover classifications were performed to facilitate future assessment of land cover change on potential spawning habitat. National Agriculture Imagery Program (NAIP) 1-m spatial resolution data were downloaded from the Texas Natural Resource Information System's website (<https://TNRIS.org>) for years 2004, 2008, and 2012 for Calhoun, Victoria, Dewitt, Gonzales, and Refugio counties. The data consist of color infrared dataset compressed county mosaics with a 1-m spatial resolution. The only exception was for Dewitt County, which did not have a county mosaic for 2004, so one was created by downloading the individual quarter quadrangles and mosaicking them together. Image preprocessing included clipping the compressed county mosaics to the 100-year floodplain and projecting the data to WGS84, UTM 14N. For each year, the separate county mosaics were merged together to create a continuous dataset of the study area.

A maximum likelihood supervised classification was performed on each year of imagery. Spectral signatures, representative of five land cover classes, were collected throughout the study area: water, barren/developed, closed canopy, agriculture/herbaceous, and wetland. Multiple signatures per land cover class were collected to represent geographic and spectral variation in reflectance for the various classes. After classification, the classes were recoded to combine similar output classes where thematic land cover was assigned the following codes: water (10), barren/developed (20), closed canopy (30), agriculture and herbaceous (40), and wetland (70) (Figures 23-25).

Pixel-based classifications of moderate-to high-resolution imagery tend to exhibit speckling of land cover (i.e., a salt-and-pepper appearance). To mitigate this effect, a 7x7 neighborhood function was applied to the output classifications to reassign the output using a majority rule. Prior to quantitative accuracy assessment, we qualitatively assessed the output classifications to determine if gross misclassifications were present in the outputs. For areas that exhibited obvious misclassification, we converted the raster data to polygon, recoded to the correct classification, converted back to raster, and re-merged with the original classification.

Post classification accuracy assessments used 1,000 assessment points distributed across the study area using a stratified random strategy. Overall accuracies were relatively low, which is not uncommon for high resolution image classification. Error matrices for the image classifications as well as accuracy assessments are provided below in Tables 4 and 5.

Table 4. a.-c.: Error matrices showing misclassified pixels for a.) 2004, b.) 2008, c.) 2012.

a.)	2004 Error Matrix	Reference					
		Water	Barren/ Developed	Closed Canopy	Agriculture/ Herbaceous	Wetland	Grand Total
Classified	Water	133		2		1	136
	Barren/Developed	2	10	8	7	11	38
	Closed Canopy	6	1	210	17	79	313
	Agriculture/ Herbaceous	3	9	23	150	90	275
	Wetland	2	2	40	65	129	238
	Grand Total	146	22	283	239	310	1000

b.)	2008 Error Matrix	Reference					
		Water	Barren/ Developed	Closed Canopy	Agriculture/ Herbaceous	Wetland	Grand Total
Classified	Water	115		2	1	9	127
	Barren/Developed	3	3	1	6	4	17
	Closed Canopy	9	1	216	40	92	336
	Agriculture/ Herbaceous	5	9	17	126	70	227
	Wetland	14	5	47	65	140	271
	Grand Total	146	18	283	238	315	1000

c.)	2012 Error Matrix	Reference					
		Water	Barren/ Developed	Closed Canopy	Agriculture/ Herbaceous	Wetland	Grand Total
Classified	Water	111		3		6	120
	Barren/Developed	1	4		6	3	14
	Closed Canopy	9	1	212	23	77	322
	Agriculture/ Herbaceous	5	7	27	153	96	288
	Wetland	19	7	40	59	131	256
	Grand Total	145	19	282	241	313	1000

Table 5 a.-c.: Accuracy assessments for each year, a.) 2004, b.) 2008, c.) 2012.

**a.) 2004 Accuracy Assessment**

Overall Accuracy 63.20%  
 Kappa Coefficient of Agreement 0.51

Class	Producer	User	Kappa
Water	91.1	97.8	0.97
Barren/Developed	45.5	26.3	0.25
Closed Canopy	74.2	67.1	0.54
Agriculture/Developed	62.8	54.6	0.40
Wetland	41.6	54.2	0.34

**b.) 2008 Accuracy Assessment**

Overall Accuracy 60.00%  
 Kappa Coefficient of Agreement 0.46

Class	Producer	User	Kappa
Water	78.8	90.6	0.89
Barren/Developed	16.7	17.6	0.16
Closed Canopy	76.3	64.3	0.50
Agriculture/Developed	52.9	55.5	0.42
Wetland	44.4	51.7	0.29

**c.) 2012 Accuracy Assessment**

Overall Accuracy 61.00%  
 Kappa Coefficient of Agreement 0.48

Class	Producer	User	Kappa
Water	76.6	92.5	0.91
Barren/Developed	21.1	28.6	0.27
Closed Canopy	75.2	65.8	0.52
Agriculture/Developed	63.5	53.1	0.38
Wetland	41.9	51.2	0.29

Considerable confusion is present between several land cover classes for all years. Specifically, classification confusion between closed canopy and wetland as well as agriculture/herbaceous and wetland are present for all three years of classified data. Although errors of commission and omission between agriculture/herbaceous and wetland are not too concerning since they both provide suitable physical structure for Alligator Gar, misclassification of closed canopy and other

vegetation classes can lead to misidentification of suitable gar spawning habitat. Conditional kappa coefficients were also quite low ( $<0.55$ ) for all classes except water with closed canopy showing moderate agreement and barren/developed, agriculture/herbaceous, and wetland indicating poor agreement.

Obtaining highly accurate classifications using high-resolution imagery is challenging for many reasons. First, except for hyperspectral imagery, high spatial resolution sensors tend to have lower spectral resolution (i.e., fewer spectral classes and/or wider bandwidths). Second, NAIP imagery are acquired over a range of dates and sun-sensor geometries, which makes accounting for spectral variability of class signatures particularly challenging. NAIP data provided by TNRIS are delivered as compressed county mosaics that have been radiometrically altered to look visually pleasing, but do not retain the same radiometric integrity as the original datasets. A solution to this problem would be to obtain the original imagery and convert all scenes to at-sensor reflectance to normalize for sun angle; however, that processing was beyond the time and scope of this project. Moreover, even with radiometrically normalized data, issues with bidirectional reflectance function of materials poses a problem as differences in spectra increase with spatial resolution.

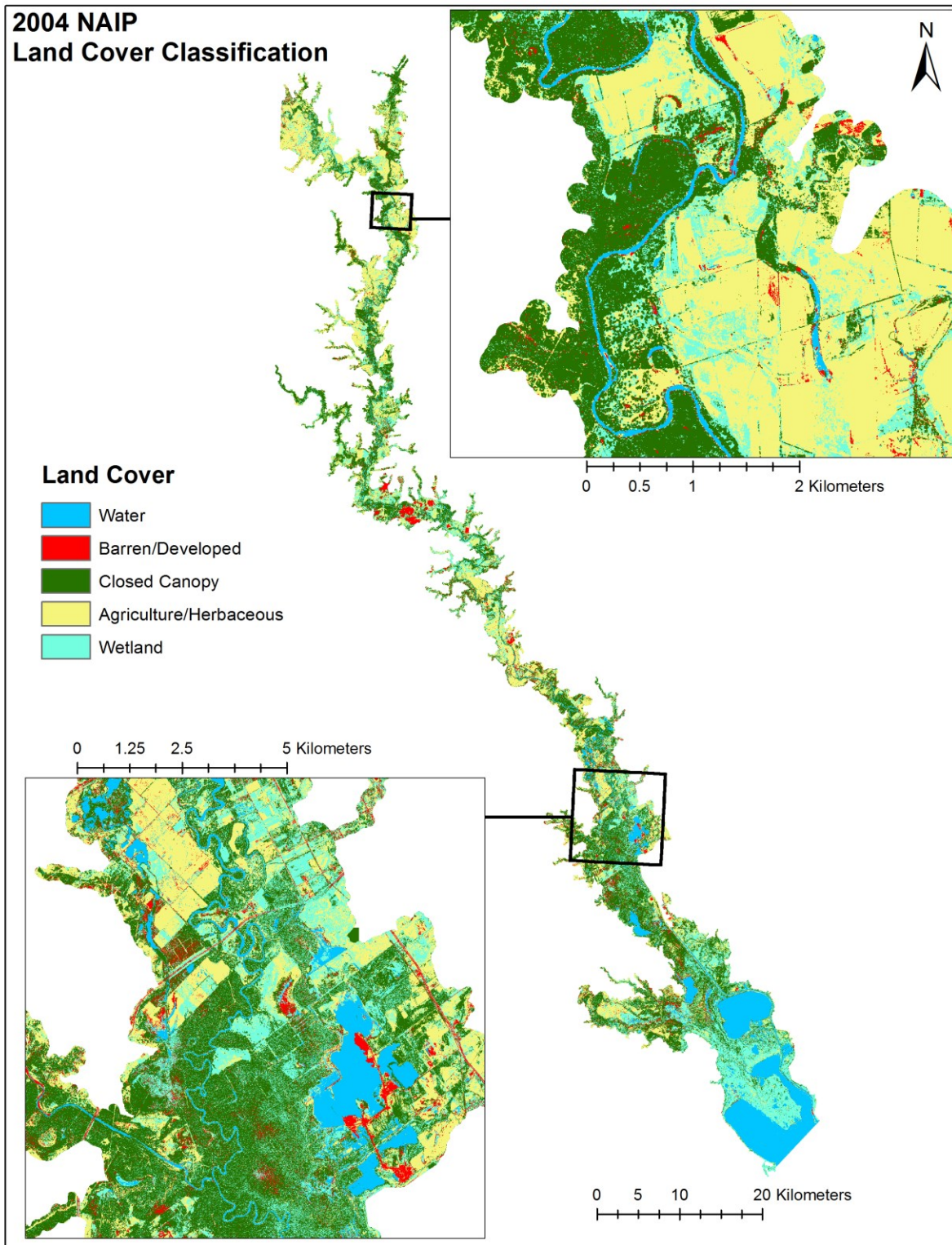


Figure 23: 2004 Land cover classification.

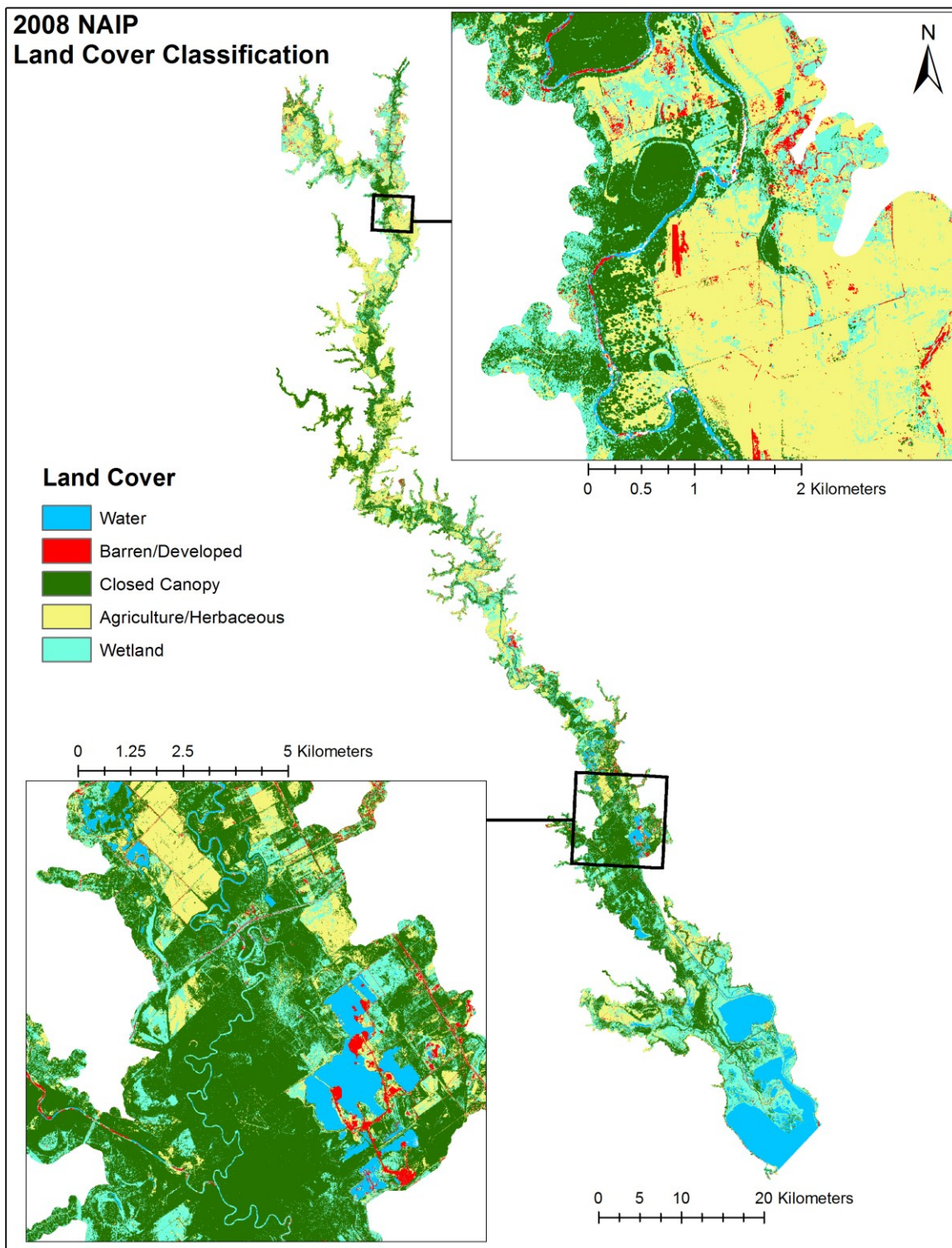


Figure 24: 2008 Land cover classification.

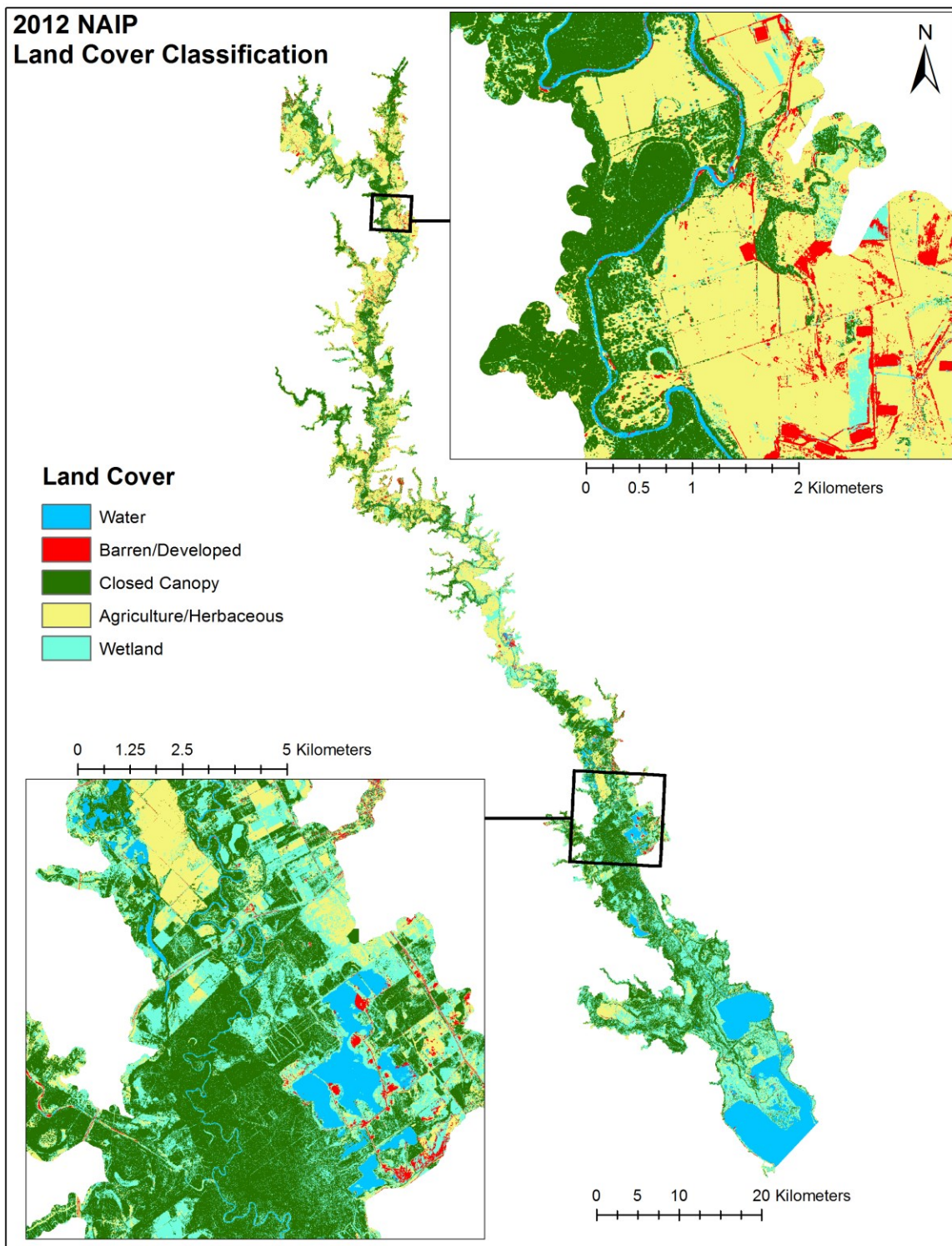


Figure 25: 2012 Land cover classification.

## **Acknowledgements**

We would like to acknowledge the following groups of people: Texas State University students Mason McGee and Keagan McNew for their assistance with this project; Texas Parks and Wildlife collaborators Clint Robertson, Kevin Mayes, and Karim Aziz for providing a list of the suitable vegetation habitat classes and feedback through the modeling process; and Texas Water Development Board collaborators Nolan Raphelt and Mark Wentzel for helpful discussions on HEC-RAS model improvements. This project was funded by the Texas Water Development Board (TWDB Contract No. 1448311791) through the Texas Parks and Wildlife Department (TPWD Contract No. 474120 with Texas State University).

## **Software Cited**

ESRI, 2017. ArcGIS Desktop, software v.10.2 and v.10.4.1 Redlands, CA., Environmental Systems Research Institute.

USACE, 2016. HEC-RAS 1D/2D. v. 5.0.1. US Army Corps of Engineers. <http://www.hec.usace.army.mil/software/hec-ras/downloads.aspx>

USACE, 2016. HEC-GeoRAS. v. 10.2 for ArcGIS 10.2. US Army Corps of Engineers. <http://www.hec.usace.army.mil/software/hec-georas/downloads.aspx>

USACE, 2016. HEC-SSP. v.2.1.1. US Army Corps of Engineers. <http://www.hec.usace.army.mil/software/hec-ssp/download.aspx>

## Appendix A

### Responses to Requested Changes to Task 1 Report

1. Please reference “TWDB Contract No. 1448311791” on the cover of the report. **revised**
2. Please check the report for typos such as the following and correct as necessary:
  - a. Page 1, 1<sup>st</sup> paragraph, 2<sup>nd</sup> sentence, “2004, 2008, 2012” should be “2004, 2008, and 2012.” **revised**
  - b. Page 16, 2<sup>nd</sup> paragraph, last sentence, “provide a spatially-explicit examples” should be “provide spatially-explicit examples.” **revised**
  - c. Page 23, 2<sup>nd</sup> paragraph, 2<sup>nd</sup> sentence, “and representative of water” should be “and were representative of water.” **revised**
  - d. Page 23, 2<sup>nd</sup> paragraph, last sentence, “herbaceous (40), wetland (70)” should be “herbaceous (40), and wetland (70).” **revised**
  - e. Page 23, 4<sup>th</sup> paragraph, last sentence, “images classifications” should be “image classifications.” **revised**
  - f. Page 25, 1<sup>st</sup> paragraph, last sentence, “showing the moderate agreement” should be “showing moderate agreement.” **revised**
3. Please use the standard abbreviation for Light Detection and Ranging (LiDAR rather than lidar) throughout the report and provide a definition before its first use on page 3, 1<sup>st</sup> paragraph, 1<sup>st</sup> sentence. **Response:** The acronym ‘lidar’ for Light Detection and Ranging is a peer-review accepted abbreviation and is becoming more common in modern use than LiDAR in the peer-reviewed literature. It is also the abbreviation that appears in Merriam-Webster dictionary. Nonetheless, per requested we changed lidar to LiDAR in the report.
4. Page 3, Table 1 lists acquisition dates for various LiDAR projects. Although factually correct, these are not of direct interest to a reader of this report. Please provide a table that lists the date of LiDAR acquisition for counties of interest to this project. For example, please explicitly provide a date when data for Gonzales County was acquired and do not reference Hidalgo County (which is well outside the area of interest for this project) in the table. **Response:** We updated the table to include the name of the counties and the dates of acquisition. Hidalgo was included previously because that is the name of the CAPCOG project which includes areas of coverage for this project, we were not implying that Hidalgo County was part of the study area, it is by default the name of the project when the data is queried from TCEQ.
5. On page 3, 3<sup>rd</sup> paragraph, 1<sup>st</sup> sentence, several of the references have a \* associated with them (e.g. (v. 5.0.1, USACE, 2016)\*). Please provide an explanation for the use of this symbol or remove it from the text. **Response:** asterisks were removed, they served no purpose.
6. Page 6, 2<sup>nd</sup> paragraph, 2<sup>nd</sup> bullet states that a *minimum* of 500 points were allowed on each line. Please check whether a *maximum* of 500 points was intended and correct as necessary. **Response:** ‘maximum’ was intended, and this has been revised.
7. Page 6, Section C, Point 5 states that flows modeled included “the 2, 5, 10, 15, 20, and 50 year probability flood events.” These should be referred to as either “the 1 in 2, 5, 10, 15, 20, and 50-year return period flood events” or “the 2, 5, 6.7, 10, 20, and 50 percent annual probability flood events.” **Response:** We have corrected this throughout the report to the language “the 1 in 2-, 5-, 10-, 15-, 20-, and 50-year return period flood events”.
8. The 2<sup>nd</sup> paragraph on page 7 compares modeled water surface elevations to stage-discharge relationships from USGS gages in the project area. The model is described as underestimating flood depths by **two meters** at the Victoria gage! The report suggests that the discrepancy may

be due to a difference in datum between the Digital Terrain Model (DTM) and the USGS gage. Further, validation of the DTM is suggested as an activity for a next phase of this project. This discrepancy has to be resolved or the model, and any analysis based on the model, is of little value. Please resolve the datum issue before this report is finalized. **Response:** The error in the modeling has been resolved, new error values are reported in Table 3. We were able to reduce the error in the HEC-RAS model so that the modeled floodplain water surface elevations are much more accurate (within centimeters). This required changing the extent of the model, reconfiguring the cross-section geometry, and manipulating the boundary conditions in HEC-RAS. These changes are documented in the revised report. The issue with the DTM, i.e., specifically the channel bed elevations and USGS gage datum have not been resolved. A more accurate DTM will require field-surveyed bathymetry data.

9. Please provide page numbers on the final report. **revised**
10. For the benefit of readers not familiar with the term, please consider providing a brief definition of the term “hydro-enforcement” used on page 3, 2<sup>nd</sup> paragraph, 3<sup>rd</sup> sentence. **Response:** We added in the following: “Hydrologic enforcement is the process of altering the elevation values in a DEM in order to ensure the continuous flow of water downstream. The simplest methods for filling sinks and assigning flow direction were enforced to the DTMs.”
11. For ease of reading and comparing values, please consider right justification for numbers in tables throughout the report. **Response:** Revised to include right justification in tables.
12. The National Weather Service (NWS) provides inundation mapping near the Victoria gage (<http://water.weather.gov/ahps2/inundation/index.php?gage=vict2>). The NWS website provides water surface elevations for floods relative to North American Vertical Datum of 1988 and the stage of the gage. To allow for evaluation of the results of this project and the NWS effort, please consider adjusting the location of the inset areas shown in Figures 3-9 of the report to overlap with the area of inundation mapping provided by the NWS. Examining this area in detail may also provide insight regarding datum issues encountered by this project. **Response:** Flood depth and HSM figures include an inset that covers the area of the NWS inundation mapping near Victoria. When making comparisons of these note that the NWS maps do not include already ponded areas/existing water bodies within the floodplain as part of the flood extent, the HEC-RAS model inundates these as they are depressions below the modeled water surface elevation, so when comparing the two layers it is best to use a satellite view to take into account existing waterbodies on the floodplain, which show up as inundated on the HEC-RAS model but not the NWS flood extents (at least at lower discharges).